DIGITALCOMMONS
@WAYNESTATE

Wayne State University

Wayne State University Dissertations

1-1-2013

Human Cytomegalovirus Us17 Locus Fine-Tunes Innate And Intrinsic Immune Responses

Stephen James Gurczynski
Wayne State University,

Follow this and additional works at: http://digitalcommons.wayne.edu/oa_dissertations

 Part of the Virology Commons

Recommended Citation
Gurczynski, Stephen James, "Human Cytomegalovirus Us17 Locus Fine-Tunes Innate And Intrinsic Immune Responses" (2013). *Wayne State University Dissertations.* Paper 840.

This Open Access Dissertation is brought to you for free and open access by DigitalCommons@WayneState. It has been accepted for inclusion in Wayne State University Dissertations by an authorized administrator of DigitalCommons@WayneState.

HUMAN CYTOMEGALOVIRUS US17 LOCUS FINE-TUNES INNATE AND INTRINSIC IMMUNE RESPONSES

by

STEPHEN JAMES GURCZYNSKI

DISSERTATION

Submitted to the Graduate School

of Wayne State University,

Detroit, Michigan

in partial fulfillment of the requirements

for the degree of

DOCTOR OF PHILOSOPHY

2013

MAJOR: IMMUNOLOGY AND MICROBIOLOGY

Approved by:

_____

Advisor Date

_____

_____

_____

DEDICATION

This work is dedicated to my loving wife Laura and my son Raymond. Their love and support has been instrumental in life.

ACKNOWLEDGEMENTS

I would like to thank Drs. Thomas Shenk (Princeton University), Dong Yu (Washington University), Wade Gibson (John Hopkins University), and Kezhong Zhang (Wayne State University School of Medicine) for generously sharing recombinant viruses, antibodies, and qRT-PCR facilities. The members of the Pellett lab, including, my advisor Dr. Phil Pellett, Dr. Subhendu Das, Daniel Ortiz, and William Close for help and support over the years. I also thank the Applied Genomics Technology Center (AGTC) at Wayne State University for RNA analysis and hybridization onto the HT-12 beadarrays. This work was supported by NIH grants 1 R56 AI099390-01, R03 AI076568-01, and R21 AI076591-01.

TABLE OF CONTENTS

LIST OF FIGURES

Chapter One

General Introduction

Human herpesviruses, organization and replication. Human herpesviruses (HHV) are a family of diverse, enveloped, double stranded DNA viruses. Widely distributed amongst the population, herpesviruses are divided into three main subfamilies; alphaherpesviruses including herpes simplex virus (HSV) 1 and 2 as well as varicella zoster virus (VZV). Betaherpesviruses which includes human cytomegalovirus (HCMV), HHV-6 A and B, as well as HHV-7. Finally, gammaherpesviruses which includes Epstein Barr virus (EBV) and Kaposi's sarcoma-associated herpesvirus (KSHV). Herpesviruses are associated with a wide range of disease in humans that range from mild and self-limiting to life threatening. HHV1 and 2 are the causative agents of cold-sores and genital blisters while VZV causes chicken pox. Infections with HCMV and EBV can result in infectious mononucleosis. HHV-6B is responsible for the febrile illness roseola infantum. Additionally two HHVs are known to be oncogenic, EBV is associated with various cancers of the throat and naso-pharynx including Burkitt's lymphoma while KSHV causes Kaposi's sarcoma.

All herpesviruses share a common structure consisting of an icosohedral nucleocapsid containing a large double stranded DNA genome. Surrounding the nucleocapsid is an amorphous, semi-ordered (1), protienacious layer termed the tegument which serves as an arsenal of pre-synthesized proteins that herpesviruses can use during the very earliest stages of infection to modulate host immune responses and trans-activate viral gene expression. Surrounding the tegument is a host membrane derived lipid envelope studded with various viral glycoproteins important for both attachment to and fusion with the host plasma membrane. The genomes sizes of herpesviruses range from the smallest ~125 kpb in VZV to the largest, HCMV, which possesses a ~236 kbp genome.

Although cellular tropism and associated disease varies between different subfamilies of herpesviruses, all share a common life cycle. Infection begins with attachment to the host cell plasma membrane by way of interaction with heparin sulfate proteoglycans and cell specific cellular receptors with various viral glycoproteins, chiefly gB (2,3). Cellular receptors vary between HHV species. For instance, HSV1 binds to a member of the tumor necrosis factor family of receptors termed HVEM (4) while HCMV binds to various cellular integrins (α2β1, α6β1, and αVβ3) in fibroblasts (5) while binding to epithelial growth factor receptor (EGFR) to gain entry into macrophage (6). Penetration of the nucleocapsid is achieved through either direct fusion with the plasma membrane or pH dependent endocytosis (7,8). As the virions enters the host cell various tegument proteins are released from the virion structure into the cytoplasm where they act in various roles including host cell immunomodulation, host cell protein synthesis modulation, and viral gene transactivation (9). The nucleocapsid is then transported, via microtubules, to the cytoplasmic edge of the nucleus where the genome is injected (10). This is the start of what is termed the lytic replication process which results in an ordered series of viral gene products and viral genome replication resulting in the production of progeny infectious virus.

The first series of viral genes produced during the lytic gene cascade are termed immediate early genes (IE) or α genes. These genes are not dependent on a priori synthesis of other viral genes or viral DNA synthesis. As α genes serve a variety of functions acting in concert with tegument proteins delivered during virion entry. Immediate early proteins 1 and 2 in HCMV are promiscuous trans-activators of many viral and host genes (11-13). Although trans-activation is a necessary step in the lytic process, α genes have various other functions. IE 1 and 2 serve a dual role as both trans-activators and immune modulators acting to suppress various aspects of host innate immunity (14). The IE gene UL37.1 acts as an anti-apoptotic protein keeping the cell alive during this critical first stage of infection (15,16). The US2 and US7

proteins in HCMV act to block expression of MHC class I bound peptides at the cell surface immediately after infection, stemming the activity of CD8+ cytotoxic T-cells (17). Thus, α genes play important roles in setting the stage for a productive lytic infection.

The second class of genes produced termed early genes, or β genes, have expression that *is* dependent on de novo protein production (α genes) but is not dependent on viral DNA synthesis. These genes are associated with viral DNA replication and include the viral DNA polymerase, and DNA processivity factor (HCMV UL54 and UL44) as well as nucleocapsid assembly factors such as the major and minor capsid proteins (HCMV UL104, and UL105). Capsid assembly takes place in the nucleus for all herpesviruses, after which, replicated genomes are packaged and the assembled nucleocapsid exits the nucleus by way of budding through the inner and outer nuclear membranes into the cytoplasm (18-21). This process of capsid nuclear egress coincides with production of a third class of late genes, or γ genes. Generally, γ genes are structural proteins, including tegument proteins, which aid in the final assembly of the complete virion.

The final phase of the herpesvirus lifecycle, termed secondary envelopment, takes place in the cytoplasm. The nucleocapsid aquires its full complement of tegument proteins as it transits through the cytoplasm to the site of envelopment and eventual egress from the cell. This process involves various organelles which differ between species of herpesvirus. Alphaherpesviruses bud into vesicles derived from the Golgi apparatus (22,23). While HCMV has been shown to use vesicles that have markers for both the trans-Golgi, and early endosomes (24,25). After budding into the exit vesicle the viral particle is then trafficked to the plasma membrane where fusion occurs releasing the virion into the extracellular space.

Primary infections with human herpesviruses generally begin with a lytic infection at the mucosal epithelium of the mouth, nose, or genitals which serve as first sites of contact. Primary

infections are generally mild and self limiting, after which viral progeny will disseminate and begin the second stage of the viral life cycle, a life-long asymptomatic infection, termed latency. All herpes viruses have the ability to establish latent infections in their hosts, although the cell types in which this happens varies between subfamilies. Latent infections are characterized by the production of very few viral antigens save for a few latent associated transcripts and proteins (26-28), the absence of the lytic gene cascade and maintenance of the viral genome as a chromatinized episome. As mentioned, cell types in which latency occurs vary and include various neuronal lineage cells for alpha herpesviruses (29,30), monocytes and undifferentiated CD34+ hematopoietic stem cells for HCMV (31,32), and memory B cells for EBV (33). Upon various stimuli, including stress, the suppression of the immune system or differentiation of the cell harboring the latent infection, reactivation to the lytic pathway can occur producing infectious virus and symptomatic disease.

HCMV background and clinical significance. HCMV is the prototypic human betaherpesvirus. Infecting 50 to 90% of the population, HCMV is the herpesvirus of largest public health concern (34). The age at which primary infection is contracted varies on a number of factors, generally increasing proportionally with age (35). Most primary infections with HCMV are mild and can result in self limiting mononucleosis similar to what is observed upon infection with EBV. After primary infection, establishment of a life-long latent infection occurs that can spontaneously and periodically reactive resulting in shedding of large amounts of virus in the saliva and urine (36-38).

HCMV presents a public health concern in two major areas. High morbidity and mortality result from HCMV infections in the immunosuppressed, either due to HIV/AIDS or immunosuppressive therapies from organ transplantation or cancer treatment. Infections in such populations can be life-threatening and result in a variety of diseases including retinitis,

gastro-enteritis, pulmonitis, hepatitis, and encephalitis and HCMV is a major cause of blindness, due to retinitis, in HIV/AIDS patients (39,40). Reactivation of HCMV is also common after organ transplantation stemming from either a pre-existing infection in the transplant patient or from reactivation of latent virus in the transplanted tissue. HCMV infection after transplantation can result in graft vs. host disease and organ rejection, and is the number one viral illness suffered by organ transplant recipients (41-43). HCMV infection drives production of HLA-E restricted CD8+ lymphocytes, many of which are specific for peptides derived from the UL40 ORF (44). These CD8+ cells are thought to play roles in both organ rejection and graft vs. host disease. During acute organ rejection recipient derived HCMV specific CD8+ lymphocytes attack endothelial cells of the donor organ that display HCMV antigens (44,45). Conversely, in graft vs. host disease HCMV specific CD8+ cells that are grafted along with the target organ facilitate immune responses in the host (45).

The second area of public health concern for HCMV involves Infections in developing fetuses and neonates. If a seronegative woman contracts a primary HCMV infection during pregnancy the virus has the ability to establish an initial infection in the placenta (46-48). This can result in cross-placental transmission to the fetus causing severe neurological sequelea including seizures, microcephaly, hearing impairment, and lifelong mental disability (49). Approximately ~1% of live births in the US are in some way affected by HCMV and it is the largest non-genetic cause of hearing loss in newborns and infants (50).

HCMV genome structure and coding capacity. HCMV has the largest genome of any human herpesvirus. At 236 kbp, it has a coding capacity consisting of at least ~170 canonical translated open reading frames (ORFs) (51,52). The number of translated ORFs has been shown to be as high as 750 when small ORFs (less than 50aa) were counted (53). HCMV also encodes 14 micro-RNAs (54-56). The genome of HCMV is divided into two major segments

termed unique long (UL) and unique short (US) each of which is flanked by sets of internal and external repeat sequences. The unique long segment contains many genes that are shared across all herpesviruses encoding proteins such as the viral DNA polymerase, major and minor capsid proteins, trans-activators, and tegument proteins. The unique short region encodes many genes that are CMV specific (57) (Fig. 1).

Interestingly, only ~40 of the 170 proteins encoded by HCMV are essential for lytic replication in primary fibroblasts (58). The remainder of the proteins that HCMV encodes for are termed accessory genes and have various functions such as immuno-modulation and cellular tropism determination. These proteins are not necessary to establish a productive infection in cell culture systems but are nevertheless important in the context of infection in a host where an intact immune system puts anti-viral pressure on the replicating virus (59). The necessity of many accessory genes is context dependent on a variety of biological conditions, i.e., MOI and cell type. In fact, the laboratory strain, AD169, which has been serially passaged in fibroblasts for decades has lost a 14 kb region of DNA termed the ULb' region. Genes encoded in this region, UL128-UL150, are completely dispensable for growth in primary fibroblasts. Several genes in this locus, namely UL128, UL129, and UL131 form a pentamer glycoprotein complex with gH and gL and are necessary tropism factors for entry into endothelial cells and epithelial cells (7). The locus UL130-UL138 in the ULb' region is also dispensable for growth in fibroblasts but is necessary for proper virion assembly/maturation and the formation of the cVAC in endothelial cells (60,61). Several other ULb' encoded genes serve immunomodulatory roles. These genes alter NK ligand cell surface expression or act as viral orthologs of cellular cytokines such as vIL-10 and vCxCL-1 (62-65). Thus, accessory genes perform critical functions under certain conditions but are dispensable for replication in the most commonly used primary fibroblast cell culture model.

Many of these accessory genes group by sequence similarity into families of related proteins (Fig. 1). These families are thought to arise from the initial capture, by way of DNA recombination, of a fully spliced host mRNA into the viral genome (57,66,67). Over successive rounds of replication these genes can be duplicated again and again on the viral genome forming a multiple member protein family. Through random mutation and evolutionary selection, members of a protein family can diverge from one another and will be preserved in the genome if they provide a selective advantage. Thus, over millennia of evolution, viral protein families can form that display large amounts of sequence diversity between constituent members and little to no sequence similarity to the original gene from which they originated.

The US12 family. One such family of related genes, termed the US12 family, is comprised of ten tandemly arranged sequence related proteins (US12-US21) located in the unique short region of the HCMV genome. Each US12 member shares a similar predicted type III transmembrane protein structure having six or seven transmembrane regions. Topology algorithms such as TMHMM which use a hidden Markov model to predict membrane spanning regions, place the N-termini of all US12 proteins in the lumen (inside) of the organelles on which they reside and the C-termini in the cytoplasm (Fig. 2). However, recent studies of Bax Inhibitor-1, a potential mammalian ortholog, showed that both the N and C termini resided in the cytoplasm with the seventh predicated transmembrane region only partially embedded in the membrane (68). Although no experimental topological data exists for US12 proteins they have been found to reside on various intracellular organelles of the host cell during infection. Antibodies against several US12 family members, including US14, US17, and US18, have localized them to membranes of organelles found in the HCMV cytoplasmic virion assembly complex (cVAC). Each member has a unique intracellular distribution and they co-localize with cellular markers of various organelles including early endosomes, cis/trans Golgi, and the

nucleus (69,70). This indicates that although they all share a common predicted structure, they may serve distinct functions during infection.

Unique to primate cytomegaloviruses, including rhesus monkey, chimpanzee, human, and gorilla, the US12 family is completely absent from CMVs of other non-primate mammals. Sequence analysis of the US12 family has revealed some similarity to cellular GPCR receptors including several members that have a DRY amino acid motif which is important for binding small G-proteins as well as C-terminal amino acid motifs which are commonly used by proteins to facilitate protein-protein interactions with various other signaling pathways including notch and WNT (71). In addition to GPCR similarity, US21, US20, US14, US15, and US17 all have amino acid motifs that could potentially classify them as members of the transmembrane bax-inhibitor-1 (TMBIM) family of anti-apoptotic and ER stress modulating proteins (71).

Phylogenetic analysis of the US12 family has revealed some interesting details of their possible origin. All US12 members separate onto their own evolutionary branch away from all other classified GPCRs and cellular signaling proteins. Each US12 family member is more similar to its corresponding ortholog in other primate CMVs than it is to any other member within the same virus species e.g., US17 in HCMV is more related to the chimpanzee US17 ortholog than it is to either US16 or US15 in HCMV, this indicates that the initial divergence of the US12 family occurred before the evolutionary split of rhesus monkeys and hominids. HCMV US21 shares the highest level of similarity with the eukaryotic protein LFG (TMBIM2) indicating that it is probably the prototypic gene that was originally captured (71)(Fig. 3).

Several studies observed cell specific phenotypes using recombinant viruses deleted for various US12 family proteins shedding light on the biological roles they may be playing during infection. Deletion of US13 from the laboratory HCMV strain Towne augmented viral growth specifically in fibroblasts by 2-logs while growth in either retinal pigmented epithelial (RPE) cells

or human microvascular endothelial (HMVEC) cells was unaffected (72). Deletion of US16 or US19 enhanced viral titers in HMVEC but not in RPE or HFF indicating that at least under certain circumstances US12 family members can act as temperance factors which slow the process of viral replication (73). A similar study carried out by Yu. et Al. using the laboratory strain AD169 showed no growth differences in HFF when any of the ten US12 family members were deleted from the laboratory strain AD169 indicating that US12 family phenotypes can be strain and cell type specific (58). When US18 was deleted from the Towne strain the virus failed to grow entirely in a cultured gingival tissue model but grew to parental titer in HFF (74). Interestingly, this virus failed to express all classes of viral genes in the gingival tissue, including IE genes, indicating a defect in the ability of the virus to bind or enter host cells and initiate infection.

Phenotypes associated with US12 family members can vary from one HCMV strain another. When US16 was deleted from the clinical isolate TR this virus failed to grow in HMVEC, a phenotype completely opposite to the one noted above when US16 was deleted from the Towne genome (75). This defect in growth was similar as to what was noted for US18 in primary gingival tissue in that the virus failed to express all classes of viral genes in endothelial cells while growing with wild type kinetics in HFF. Attachment to the plasma membrane of endothelial or epithelial cells was not altered by ΔUS16 but the mutant failed to translocate the tegument protein pp65 or viral DNA to the nuclei after infection indicating that the virus was defective for a step in the viral life cycle prior to immediate early gene expression. The underlying theme from these two studies is that deletion of US16 or US18 had the effect of modulating virion composition in such a way that these viruses grew normally in HFF but were unable to enter into and replicate various other cell types.

Consistent with this, HCMV displays broad cellular tropism (fibroblasts, endothelial cells, epithelial cells, monocytes/macrophage) and has adapted numerous strategies to enter into and replicate in various cell types. For instance, HCMV entry into endothelial and epithelial cells is mediated by the glycoprotein complex UL128-131/gH/gL and occurs through low pH endocytosis (7,76); on the other hand entry into fibroblasts is mediated by another distinct glycoprotein complex gH/gL/gO and occurs by direct, pH independent, fusion at the plasma membrane (8,77). Changes in levels of one set of glycoproteins can shift virus tropism from fibroblasts to endothelial/epithelial cells or vice versa while leaving tropism for the opposite cell type unaffected or even enhanced.

Condition specific phenotypes have also been observed following modulation of levels of tegument proteins in mature virions. A virus deleted for the tegument protein pp65 (pUL83) was highly attenuated for growth in human fibroblasts at low multiplicities of infection (MOI), but grew with wild type kinetics at high MOI (78). Further, pp65 is essential at all MOIs for growth in human macrophages and its deletion altered virion levels of the tegument proteins pUL25, pUL69, and pUL97 (79). Thus, changes in virion composition brought about by mutations to US12 family members could have marked and varied effects that are dependent on a combination of cell type and infection conditions.

The US12 family, relation to the TMBIM family of ER stress proteins. As mentioned above, US12 family members share sequence similarity with the trans-membrane bax inhibitor-1 (TMBIM) family of conserved eukaryotic anti-apoptotic seven transmembrane proteins (71). These proteins localize to membranes of various cellular organelles and are thought to act as rheostats that modulate apoptotic signaling, ER stress, and the unfolded protein response (80). ER stress is a process that is initiated by any number of cellular stressors, including viral infections, which cause a disruption to cellular homeostasis. The unfolded protein response is a

type of ER stress which results from an accumulation of unfolded proteins in the endoplasmic reticulum, in the case of HCMV, UPR results from the large amounts of viral glycoproteins produced during infection that must be correctly folded and transported through the secretory apparatus of the cell. Several members of the TMBIM family have been shown to influence intracellular calcium levels acting as pH dependent calcium channels allowing calcium to leak from the endoplasmic reticulum to the cytoplasm (81-85). Bax inhibitor-1 (BI-1 / TMBIM6) function as a negative regulator of the IRE1α branch of the UPR and over expression of BI-1 inhibits splicing of the ER stress associated transcription factor, XBP-1 that is directly processed and activated by IRE1α (86,87). BI-1 has also been shown to interact with both the anti-apoptotic protein BCL-2, and IP_3 receptors in the ER (88,89). This interaction with IP_3Rs links BI-1 with autophagic pathways and BI-1 deficient cells showed a lower resting rate of autophagic processes, however, BI-1s role in autophagy was shown to be independent of its cytoprotective functions indicating that it has multiple biological roles (90).

Another TMBIM member, human Golgi associated anti-apoptotic protein (hGAAP / TMBIM4), also influences ER Ca^{2+} levels and functions as a regulator of cell adhesion and motility (91). Interestingly, poxviruses, specifically camelpox virus and vaccinia virus, have been shown to encode orthologs of TMBIM like proteins. Termed viral Golgi-associated anti-apoptotic proteins (vGAAP) these proteins localize to the Golgi of infected cells, and are non-essential for virus growth in cell culture. Knockdown of vGAAP proteins caused an increase in lethality in a mouse model indicating that they serve as temperance factors limiting the replication or dissemination of virus in the host (92). Similar to hGAAP, vGAAP has been shown to modulate levels of calcium in the ER (93).

Clearly, TMBIM proteins have a diverse array of important functions in cell biology. HCMV is known to extensively modulate many of the pathways discussed above and it is

possible that the capture and divergence of the US12 family helps to facilitate this signaling by serving as a virally controlled TMBIM like family of proteins similar to what was observed in Poxviruses. Further, the pathways affected by TMBIM family members, i.e. ER stress and apoptosis, have been implicated as important in the processes of HCMV virion maturation and assembly. Therefore, it is highly possible that US12 family members serve as TMBIM orthologs influencing virion assembly by modulating signaling pathways important in the construction of mature virions.

Virion assembly and the cytoplasmic viral assembly complex (cVAC). At least 70 proteins have been detected in purified HCMV virion preparations (94,95) and the process of HCMV virion maturation is presently not well understood. Relying on both viral and cellular factors, cytoplasmic virion maturation is thought to occur in the cVAC, a virally induced rearrangement of the host cell secretory apparatus consisting of ordered, concentric, rings of various secretory organelles. Specifically, it consists of a region of endoplasmic reticulum at the outer edge. Just inside the ER is an interlaced ring or basket like structure consisting of membranes derived from both Golgi and trans-Golgi compartments, and a central region which contains a collection of condensed EEA1 positive early endosomes as well as a microtubule organizing center (MTOC) (96,97) (Fig. 4). The cVAC is formed from 72 to 96 hpi and corresponds with production of high levels of infectious virus and is thought to be the site of final tegumentation and secondary envelopment of maturating virions.

Many viral proteins, chiefly tegument and glycoproteins, converge in the cVAC during the late stages of HCMV infection. In fact, the cVAC was first described as a confluence of the viral tegument proteins pp28 (pUL99), pp150 (pUL32), pp65 (pUL83), the viral glycoproteins gB(pUL55), gH(pUL75), and gp65 (97,98). Since then, many other viral proteins have been shown to localize to this region including glycoproteins gO, gM, and gN, as well as the tegument

protein UL48 (99-101). While the exact function of the cVAC has not been elucidated it is clear that this structure serves as the major congregation point for many HCMV structural proteins.

Particle types produced during HCMV infection. HCMV has been shown to produce several different types of particles during infection that are able to be separated by various density gradient centrifugation techniques. The most well characterized of these is the virion with a diameter of ~250 nm consisting of the above mentioned conserved herpesvirus structure of encapsidated genome, tegument layer, and lipid envelope. Interestingly, HCMV seems to produce a very high particle to pfu ratio (i.e., the ratio of infectious units measured by plaque assay to the number of particles counted by electron microscopy) producing several hundred to several thousand non-infectious virions for every one infectious (102). These non-infectious particles are difficult to isolate and study and thus the definition of exactly which structural components are necessary to initiate a productive infection remains unclear.

HCMV also produces a particle, termed dense bodies, which are both 2 – 4 times larger and more dense than infectious virons. Dense bodies are composed mainly of viral tegument proteins with ~60% of their mass being made up of the tegument protein pp65. They possess a lipid envelope similar to infectious virions but which differs in both the abundances and types of incorporated glycoproteins (95). Dense bodies are able to enter into host cells independently of infectious virions and can deliver immunomodulatory proteins, possibly serving as “bait” particles that can elicit an immune response and thus draw host defenses away from the site of the actual infection (103). A third type of particle termed the non-infectious enveloped particles (NIEP) has also been isolated from HCMV infected cells (104). NIEP’s are essentially a genome-less capsid (B-capsid) that has undergone the process of secondary envelopment. Little is known about the possible functions of NIEPs although their lack of intact genomes most certainly renders them unable to start a productive infection.

Even though virions, dense bodies, and NIEPs are composed of essentially the same viral proteins the pathways involved in maturation of these particles differ in key areas. When viral DNA encapsidation was inhibited virions accumulated in the nucleus of infected cells but did not transit to the cytoplasm, nor were they secreted from the cell. Dense body assembly remained unaltered even in the absence of DNA encapsidation and appears to rely solely on cytoplasmic factors such as tegument protein levels (105). The viral protein UL103 was subsequently shown to be important for egress of virions, dense bodies and NIEPs indicating that while maturation pathways differ between the particle types, a common pathway is shared for particle egress (105).

Cellular pathways involved in virion assembly. Cellular proteins and pathways play a major role in both the formation of the cVAC and production of mature virions. Specifically, those involved in ER stress and the unfolded protein response (UPR) are particularly important. HCMV both induces and controls the three major branches of the unfolded protein response, PKR like ER kinase (PERK), activating transcription factor 6 (ATF6), and inositol requiring enzyme (IRE1α), activating certain aspects while inhibiting others. Various groups have shown that control of UPR pathways by HCMV is essential for both proper virion assembly and maturation. For instance, activation of PERK generally results in protein translation attenuation by way of phosphorylation of eIF2a. Although HCMV infection results in an increase in PERK phosphorylation and phospho- eIF2a, translation is not attenuated (106). Additionally, HCMV infection induces IRE1α phosphorylation and splicing of the down-stream transcription factor XBP1, but inhibits the production of XBP1 associated UPR related gene products important for ER associated protein degradation (106). Consistent with this, chemicals that specifically cause ER stress, such as thapsigargin, reduce the levels of infectious virus produced by inhibiting the final steps of virion maturation and secondary envelopment (107). Thapsigargin inhibits the ER Ca^{2+} ATPase, SERCA, thus increasing cytosolic levels of Ca^{2+} causing ER stress and eventually

apoptosis. It is not clear why the rise in cytosolic Ca^{2+} caused by thapsigargin treatment renders HCMV infected cells unable to produce progeny virions. The cells do not undergo apoptosis, as the viral protein pUL38 blocks thapsigargin inhibits apoptosis (108), but are specifically inhibited for steps in secondary envelopment. Together, these data suggest that HCMV modulates ER stress pathways in a complicated fashion inducing certain aspects while blunting others. These pathways must be regulated in a precise fashion as slight perturbations can have negative impacts on viral replication.

HCMV also specifically regulates levels of another important ER stress protein HSPA5 (AKA GRP78 or BIP). BIP is normally found in the ER where it forms a complex with other chaperones that acts to correctly fold proteins (109). HCMV increases BIP expression from 24 to 72 hpi but reduces levels at 96 hpi (110). When BIP was depleted during infection HCMV capsids could exit the nucleus but failed to migrate to the cVAC for final tegumentation and envelopment (111). Subsequently, BIP was found to localize to both the ER and to the cVAC during HCMV infection and abrogation of BIP expression during infection disrupted the structure of the cVAC causing the mislocalization of viral tegument proteins and glycoproteins (112). Thus it is evident that HCMV specifically controls expression of certain UPR and ER stress proteins to facilitate proper virion assembly and replication.

This work. Interestingly, ER stress and UPR pathways which are important for virion maturation and egress are the same pathways modulated by the TMBIM family of proteins which share homology with the US12 family. This link has not been explored and the US12 family remains an understudied, but potentially important aspect of HCMV biology. Cell specific phenotypes have been observed with US12 family mutants. However, definitive functionality has not been ascribed to any member. Constituting ~4% of the entire genetic content of HCMV (~9 kbp), the US12 family is highly conserved with all strains of HCMV thus far sequenced

containing the full complement of ten proteins. Additionally, they are 95-99% conserved at both the nucleotide and amino acid level in laboratory strains of HCMV, such as Towne and AD169 which have lost large sections of their genomes due to serial passage in fibroblasts, and low passage clinical isolates such as TB40e and FIX (51). This high level of conservation under all growth conditions and across multiple strains of HCMV indicates that members of the US12 family serve fundamentally important roles during infection. Retention of these proteins appears to provide an advantage under both cell culture conditions and during infection in a host where an active immune system places additional pressure on the virus. Thus, the study of US12 family members is paramount to a complete understanding of HCMV-host cell interaction. The following body of work sheds light particularly on one member, US17, and its role in both viral assembly and host cell immunobiology.

To further elucidate biological roles of US12 family members we have conducted microarray transcriptional profiling of cells infected with a recombinant HCMV deleted for US17 (ΔUS17). In comparison to parental virus, ΔUS17 elicited a much weaker innate and interferon response from the host cell at very early times after infection (12 hpi) producing lower levels of transcripts of pro-inflammatory chemokines and cytokines as well as those involved in type I interferon responses. This blunting of the immune response happened in the absence of US17 expression and was opposite what was seen during infection with a recombinant virus deleted for the immunomodulatory tegument protein pp65 (pUL83) (113,114). This led to the hypothesis that virions produced by ΔUS17 differed from those produced by the parental virus. Although ΔUS17 produced equal numbers of infectious particles in fibroblasts compared to its parent, at equal multiplicities of infection, it produced >3-fold more non-infectious viral particles, and delivered increased amounts of pp65 to newly infected cells. Relative to its parent, at later time points (96 hpi) ΔUS17 infected cells displayed aberrant expression of several host ER stress response genes and chaperones, some of which are important in the final stages of virion

assembly and egress. Our results suggest that US17 modulates host pathways to enable production of virions that elicit an appropriately balanced host immune response.

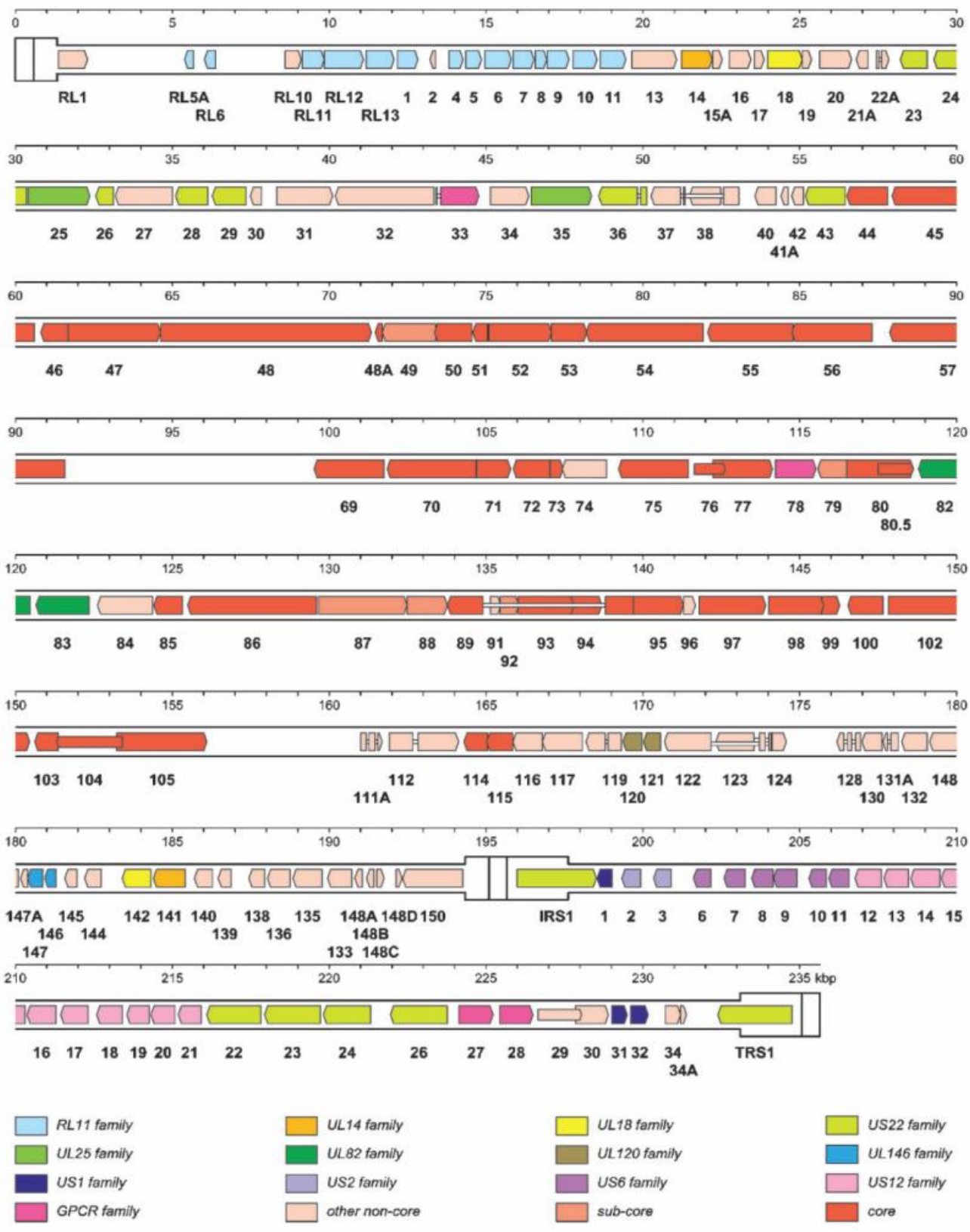

Figure 1. **Genome map of HCMV strain Merlin.** Open reading frames are depicted as colored boxes. Similarity colored ORFs are gene families.

Used with permission, from Dolan et al. Journal of General Virology (2004), 85, 1301–1312

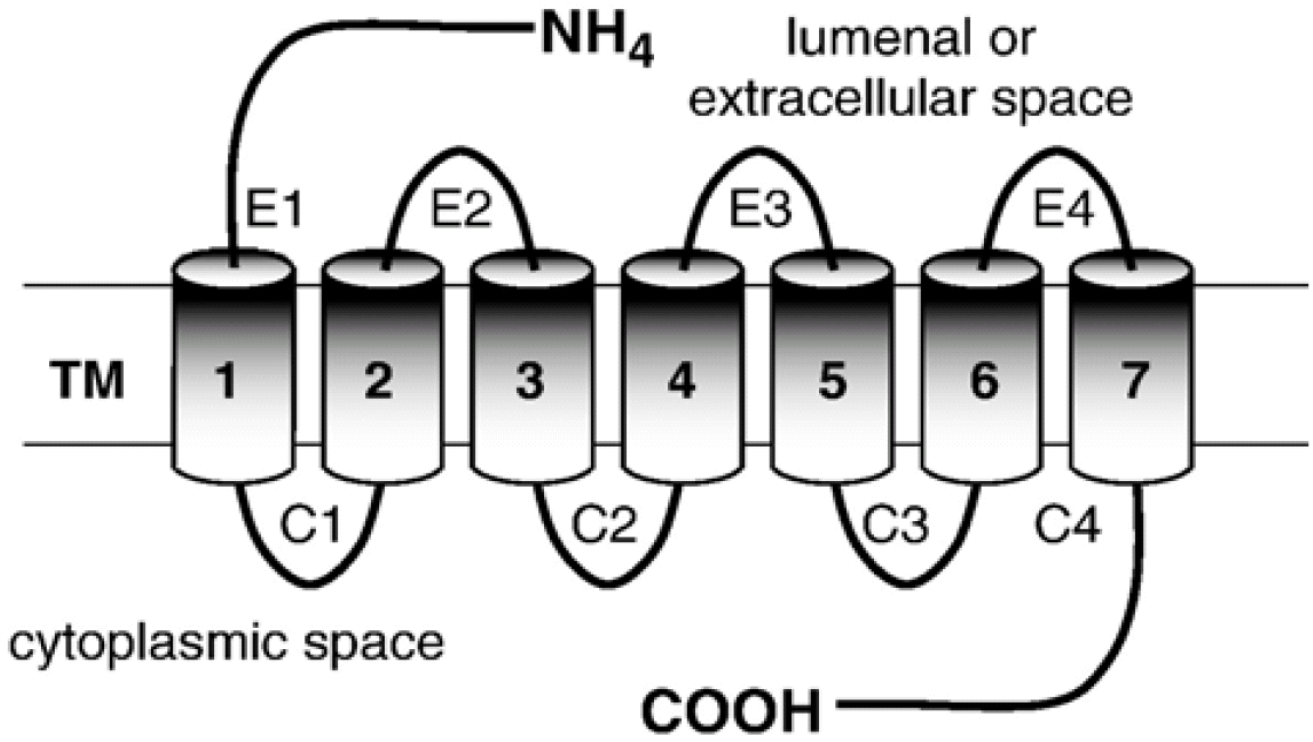

Figure 2. **Predicted structure of US12 family proteins.**

Used with permission, from Lesniewski et al. Virology (2006), 354, 286 - 298

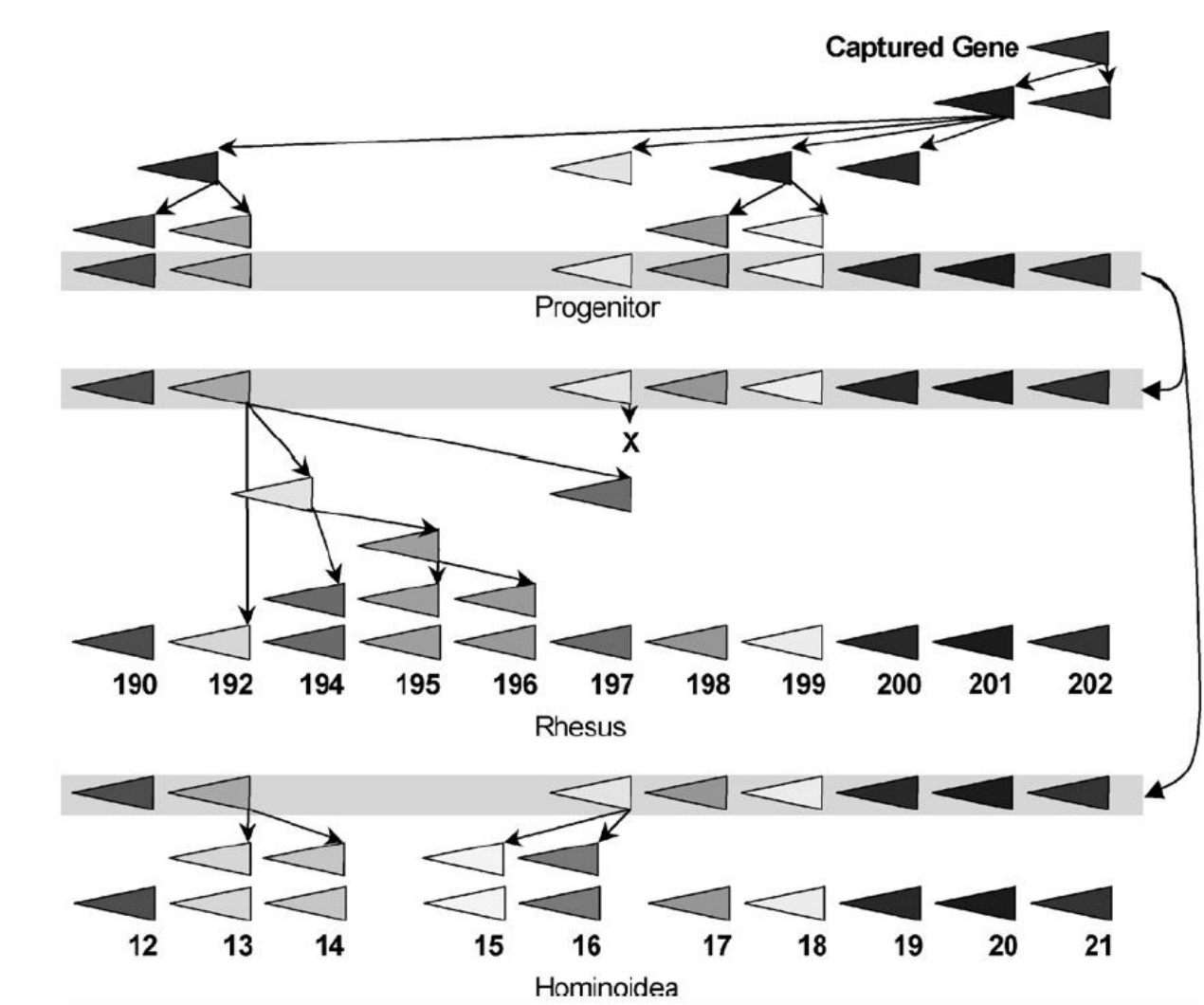

Figure 3. **Duplication and divergence of the US12 gene family.**

Used with permission, from Lesniewski et al. Virology (2006), 354, 286 - 298

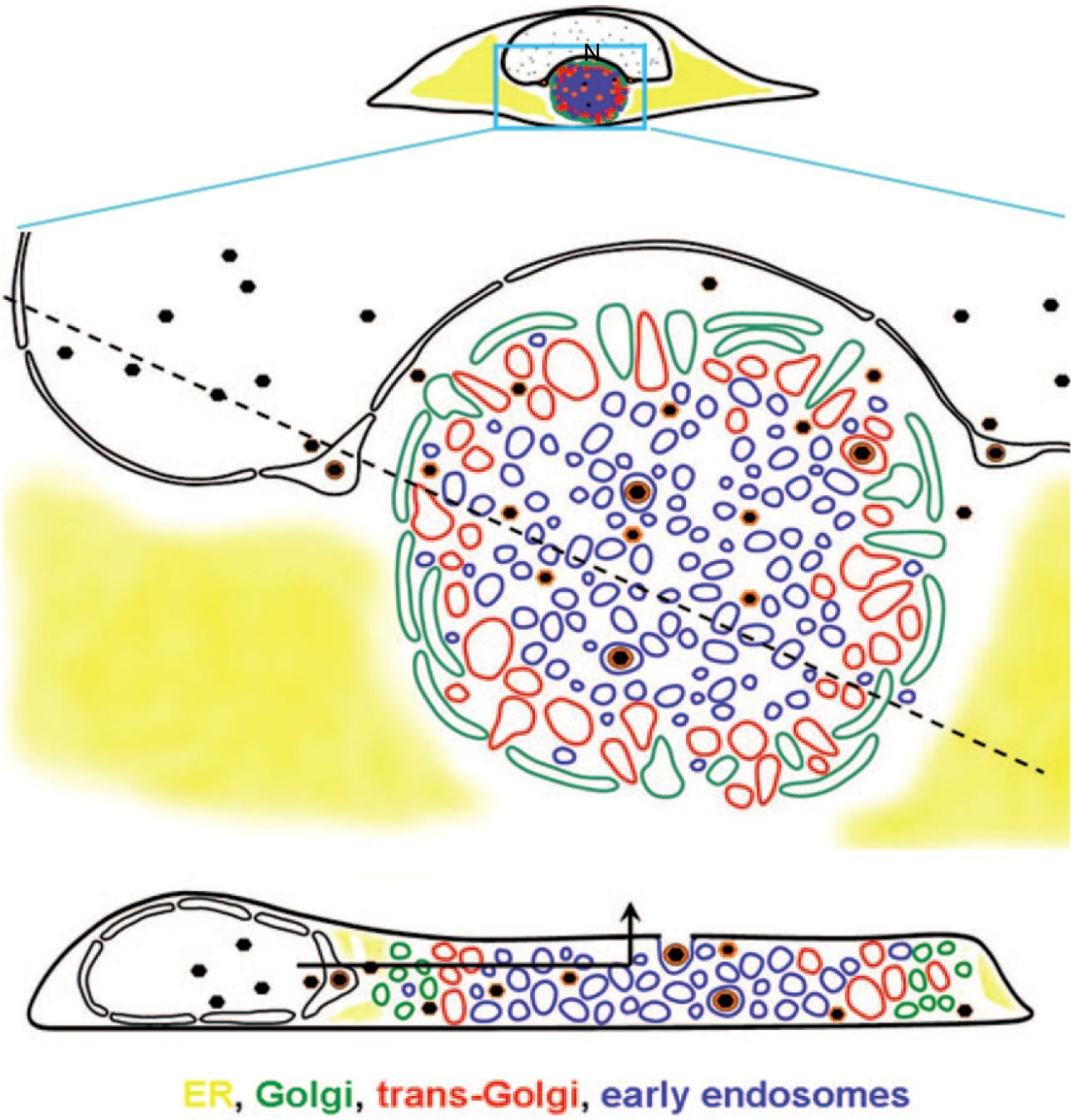

Figure 4. **The HCMV cVAC and proposed path of virion egress.** Schematic showing the cyto-architecture remodeling induced by HCMV. N indicates the nucleus with a characteristic reniform shape seen in HCMV infected cells. Multicolored shapes show vesicles of various organelles that rearrange to form the cVAC. The dashed line indicates the cut along the bias that is shown in the bottom projection. The arrows indicate the proposed path of virion egress from the interior of the nucleus through the cVAC to the central early endosome rich region.

Used with permission, from Das S. et al. J. Virol. (2007), 81(21), 11861-9

Chapter Two

Cellular transcriptional profiling of ΔUS17 infected fibroblasts

Introduction.

The multi-protein nature of the US12 family has made study of individual members difficult. It is unknown whether members can functionally complement each other thereby mitigating discernible phenotypes when any particular member is deleted or mutated. Potential complementation, coupled with the dispensability of US12 family members for growth in the most commonly used cell culture models of HCMV has greatly hampered study of the US12 family. Currently, there are no functions ascribed to any of the US12 family members and these proteins remain an untapped and potentially important area of study.

To further address the biological importance of US12 family members we have performed cellular transcriptional analysis of cells infected with a recombinant HCMV deleted for one member, US17. We previously found that US17 is expressed with late gene kinetics, and localizes to the nucleus of infected fibroblasts beginning at 72 hpi. When imaged by immunofluorescence microscopy using a polyclonal antibody directed against a C-terminal epitope, interestingly, there was little co-localization between the N and C termini of US17 when both were imaged simultaneously. Immunoblotting with the polyclonal antibody revealed that two distinct species of US17 were present in infected cells, an ~80 kDa species and a smaller ~10 kDa species indicating that US17 is expressed in a segmented fashion (70). The biological implications of this segmentation have not been elucidated and no biological function has been ascribed to US17.

Analyzing cellular pathways perturbed by deletion of US17 is an effective way to glean information about what roles it may be playing during infection. However, the limited information

available regarding the cellular roles of US12 family members makes generation of any specific hypothesis, as to which genes they may be affecting, difficult. Therefore we have opted to take an unbiased approach to transcriptional profiling.

Here we present data from an Illumina HT-12 v4 bead array from cells infected with ΔUS17 and the laboratory strain of HCMV from which the deletion mutant was derived, AD169. The HT-12 v4 is similar to a traditional microarray in that it measures expression levels of mRNA transcripts from a sample of isolated whole cellular RNA. However, several benefits are conferred by the platform over other methods of whole transcriptome analysis. The HT-12 v4 beadarray consists of 47,232 individual probes that give specific expression information for 39,809 coding sequences with well-defined or provisional annotations in the NCBI database as well as 3,961 non-coding sequences. This high number of probes provides excellent coverage and gives gene expression information for essentially every known annotated human transcript allowing for robust downstream analysis of biological pathways affected by ΔUS17. Thus we generated comprehensive cellular transcription profiles that have allowed us to elucidate a potential role for US17 even in the absence of a differential growth phenotype.

Materials and methods

Cell culture, preparation of virus stocks, and virus purification. All experiments in this study used normal human foreskin fibroblasts (HFF). All cells were used between passages 10 and 15. Cells were cultured in DMEM (Hyclone/Thermo-Fischer, Waltham, MA) supplemented with 10% fetal bovine serum, 1% penicillin/streptomycin, 1% Glutamax (Life Technologies Grand, Island, NY), and 1% minimal non-essential amino acids. HCMV strain AD169 (ATCC), the AD169 BAC pAD/Cre parental (provided courtesy of Dr. Dong Yu), and the US17 deletion virus (ΔUS17) were cultured by inoculating confluent HFF monolayers at an MOI of 0.001. Infected cells and supernatants were harvested 14 dpi and virus titers were determined by plaque assay on confluent HFF monolayers. For all experiments, low passage HFF were seeded onto 35 mm dishes 72 hr pre-infection at $3x10^4$ cells/cm^2. Where applicable, virions were concentrated by centrifugation of clarified supernatants through a 20% sorbitol cushion at 60,000 x g for 1 h in a Beckman SW 41 Ti rotor. Subsequent purification of virions was carried out by centrifuging concentrated virus through a 10-50% linear Nycodenz gradient for 2 h at 110,000 x g in a Beckman SW 41 Ti rotor (95).

Recombinant viruses. A virus deleted for the entire US17 open reading frame was constructed using a bacterial artificial chromosome (BAC) system (115). In short, E. coli (strain EL250) which harbors a temperature inducible lambda pro-phage RED recombinase for homologous linear recombination and an additional arabinose inducible FRT recombinase was transformed with a BAC of HCMV strain AD169 pAD/Cre DH18 (provided courtesy of Dr. Thomas Shenk), which is a full length BAC clone of HCMV strain AD169 that harbors a transposon insertion cassette that disrupts the US17 open reading frame (58).

An insertion cassette was created by PCR amplification using a set of primers(forward: ATCGCCACCGCCGTCgaagttcctattctctagaaagtataggaacttcAGACGTCAGGTGGCACTTTT;

reverse:AACGACGAGTTTTTCCGgaagttcctatactttctagagaataggaacttcAGCTCTTGATCCGGCAAAC) consisting of a 5' portion encoding for 15-17 bp of DNA directly flanking the US17 open reading frame upstream of the start codon or downstream of the stop codon (capital letters), an inner portion encoding a FLP recombinase site (lower case letters), and 20 bp at their 3' ends complementary to the ampicillin resistance gene of plasmid pPur (underlined) (Clontech, Mountain View, CA). A second round of amplification used the product of the first reaction as template and a set of primers consisting of 50 bases flanking the US17 open reading frame (upstream primer: ACACTCTATAAACGGTTTCTCATACGCGCCTTTTGATCGCCACCGCCGTC; downstream primer: TTGGTGGAGACGGCCGGCGCGGCGGGTGGGGGAAACGACGAGTTTTTCCG). The resulting cassette thus consisted of an inner core ampicillin resistance gene flanked by two FLP recombinase sites with 50 bp of US17 ORF flanking DNA to facilitate linear recombination.

BAC-containing E. coli was shifted to 42°C for 15 min to activate the RED recombinase, and then transformed with 300 ng of gel purified PCR product. Recombinants were selected on LB agar plates containing 25 μg/ml ampicillin, and insertion of the cassette was confirmed by HCMV genome restriction digestion with Hind III, and PCR from both within and outside the US17 ORF. To remove the cassette and generate the final in frame deletion mutant, an overnight culture of the previously described E. coli carrying the HCMV BAC and ampicillin resistance gene cassette in place of the US17 ORF was subcultured 1/50 in fresh LB media and incubated at 32°C until the culture reached OD600 = 0.5. Sterile arabinose was added to a final concentration of 0.1% and the culture was incubated at 32°C for an additional hour to activate the FLP recombinase. Serial dilutions were plated on non-selective media, colonies were picked and screened for sensitivity to ampicillin, and the deletion was verified by Hind III digestion. US17 mutants were further verified by PCR from both within and across the US17

open frame to confirm the absence of the ORF. The resulting mutant was deleted for the US17 ORF leaving only a 34 bp FLP scar.

To construct the US17 repair virus with a C-terminal V5 epitope tag, a scar less GalK recombineering system was used (116). The US17 sequence from the AD169 genome was PCR amplified using a set of primers that added the V5 epitope tag to the C-terminal end (Forward primer: TGTGGATCC**ATG**TCTCCGAACTCA, Reverse primer TTCTCGAG**TTA**CGTAGAATCGAGACCGAGGAGAGGGTTAGGGATAGGCTTACCCGCCATG GTTCGCGTGAG Bold text represents start or stop codons, underlined text represents the V5 epitope sequence.) The amplimer was cloned as a BamHI / XhoI fragment into the PCDNA3.1 vector (Life Technologies, Grand Island, NY). Next, a GalK Kanamycin resistance cassette containing 50 bp of up-stream and down-stream homologous US17 sequence was PCR amplified from the plasmid C255 (117) (provided courtesy of Dr. Dong Yu) (Forward primer: **TTGGTGGAGACGGCCGGCGCGGCGGGTGGGGGAAACGACGAGTTTTTCCG**CCTGTTGA CAATTAATCATCG, reverse primer: **ACACTCTATAAACGGTTTCTCATACGCGCCTTTTGATCGCCACCGCCGTC**CTCAGCAAAA GTTCGATTTA. Bold text represents homologous AD169 sequence; non-bold text represents the GalK/Kan^r binding sequence.) This sequence was recombined into the ΔUS17 locus using RED mediated recombination as described for the deletion mutant. Finally, the GalK/Kan^r was removed and replaced with the US17 C-terminal V5 sequence by constructing an amplimer consisting of the US17-cV5 sequence with 50 bp of homologous US17sequence at either end (Forward primer: **TTGGTGGAGACGGCCGGCGCGGCGGGTGGGGGAAACGACGAGTTTTTCCG**TTACGTAG AATCGAGACCGAGGA, reverse primer: **ACACTCTATAAACGGTTTCTCATACGCGCCTTTTGATCGCCACCGCCGTC**ATGTCTCCGA ACTCAGAGGCCAC).

Protein analysis: immunoblotting and silver staining. At the indicated time points, infected cell monolayers (MOI = 3.0) were washed once with ice cold PBS and lysed in RIPA buffer (150 mM NaCl, 10 mM HEPES [pH 7.4], 1% Noniodet P40, 1% sodium deoxycholate, 0.1% SDS, 1x protease inhibitors (Roche, Indianapolis, IN)). After incubation for 5 min on ice, lysates were clarified by centrifugation at 10,000 x g for 10 min at 4°C. Protein concentrations were measured by BCA assay (Thermo Fisher, Waltham, MA); equal amounts of total protein from each lysate, or protein from gradient purified virus fractions were run on 10% polyacrylamide gels. Silver staining of polyacrylamide gels was carried out using a Pierce silver stain kit (Thermo Scientific, Rockford, IL). Immunoblots were transferred to 0.1 µm nitrocellulose membrane and then probed with antibodies against the following proteins: IE1 & IE2, pp28, gB (Virusys, Taneytown, MD), pp65 (Fitzgerald Industries**,** Acton, MA), gH (Santa Cruz Dallas, TX), and a polyclonal rabbit antibody against the C-terminus of UL48 (a gift from Dr. Wade Gibson). Chemiluminescence was performed with Super Signal Pico West substrate (Thermo, Waltham, MA) following the manufacturer's directions.

Isolation of viral DNA or total cellular RNA for genome quantitation, microarrays, and qRT-PCR analysis. To ensure accurate multiplicities of infection, one dish of cells was trypsinized and counted immediately prior to infection to gauge final cell density. HFF (p12) were then infected with either AD169 or pAD/CRE(ΔUS17) (MOI = 6.0) for 12 or 96 hr. After washing once with PBS, 1 ml of Trizol (Life Technologies, Grand Island, NY) reagent was added to each 35 mm dish. RNA was separated by addition of 200 µl chloroform to each 1 ml Trizol sample followed by centrifugation at 12,000 x g for 15 min at 4°C. The aqueous phase was transferred to a clean tube and RNA was precipitated by addition of 500 µl of 100% isopropyl alcohol followed by centrifugation at 12,000 x g for 15 min at 4°C. The RNA pellet was washed twice in 70% ethanol and then resuspended in 50 µl of nuclease free deionized water. DNase I treatment was conducted with 2 U of RNase free DNase (New England Biolabs, Ipswich, MA)

following the manufacturer's directions. RNA concentration was measured by UV spectroscopy (260 nm : 280 nm) using a NanoDrop 1000 spectrophotometer (Thermo-Fisher, Waltham, MA). RNA quality was assessed on an Agilent Biolyzer (Agilent Technologies Santa Clara, CA); all samples had RIN values of 8 to 10. RNA was then hybridized on Illumina HT-12 v4 human bead array chips. RNA quality assessment, chip hybridization, and array reading were performed at the Wayne State University Advanced Genomics Technology Center.

cDNA for qRT-PCR analysis was generated from 1 µg of total isolated RNA using an iScript first strand cDNA synthesis kit (Bio-Rad, Hercules, CA). Equal volumes of cDNA were analyzed for all viruses using a custom Taq-man array (Applied Biosystems/Life Technologies, Grand Island, NY) and the following pre-designed primer/probes sets: GAPDH (Hs02758991_g1), IFNB1 (Hs01077958-s1), ISG15 (Hs00192713_m1), CCL5 (Hs00174575_m1), CXCL10 (Hs00171042_m1), IL6 (Hs00985639_m1), and TNFSF10 (Hs00921974_m1). An ABI 7500 fast thermocycler (Applied Biosystems/Life Technologies, Grand Island, NY) with the cycling protocol supplied with the custom array.

Isolation of viral genomic DNA from cell culture supernatants was carried out using a QIAamp MinElute Virus Spin Kit following the manufacture's direction. Supernatants were first clarified at 1000 rpm for 10 m and DNase treated with 2 U / 200 µl supernatant of DNase I(New England Biolabs, Ipswich, MA) for 10 m. Quantitation of viral genomes was done using a Syber-green based assay with primers specific for the HCMV UL83 ORF (forward primer: GCAGCCACGGGATCGTACT, reverse primer: GGCTTTTACCTCACACGAGCATT). Data was collected on a Bio-Rad MyIQ real-time thermocycler (40 cycles, 95 ºC for 15 s and 60 ºC for 1 min).

Bioinformatic analysis. Microarray analyses were performed using BRB-ArrayTools (v. 4.2.0 beta 2) developed by Dr. Richard Simon and the BRB-ArrayTools Development Team.

Differential gene expression analysis was conducted using the significance analysis of microarray (SAM) (118) option in BRB array using a false discovery rate of 0.001. Lists of significantly differently expressed genes were generated for each mutant compared to AD169 at each respective time point and expression values for these genes were then analyzed for other pairwise comparisons (mutant vs. mock, AD169 vs. mock, etc.). Gene ontology categorization of differentially expressed genes was carried out using Cytoscape v. 2.8.1 and the biological gene ontology plugin, BiNGO (119). Gene ontology definitions and annotation files were downloaded from http://www.geneontology.org/ and dated 01/19/2012. Genes were grouped based on gene ontology biological function and only over-represented categories where $P<0.0001$ were considered relevant for this study.

Results

Deletion of the US17 ORF does not significantly alter viral replication in primary fibroblasts. A BAC mutant (ΔUS17) was constructed in which the entire US17 ORF was replaced with a 32 bp frt scar (Fig. 5). This mutation did not alter the mapped polyA signal shared by US18, US19, and US20 (120), and we verified US18 expression by immunofluorescence with a previously described antibody (70). The deletion is likely upstream of transcriptional signals for US16. This mutation deletes the C-terminal 68 aminio acids of open reading frame cORF29 (RASCAL) (121). Expression of this protein was verified in strains Towne and TB40e, but not AD169. No evidence of RASCAL expression was found in a detailed translational analysis of cells infected with HCMV strain Merlin (53). In this same analysis, one expressed ORF was identified that is expressed from an alternative translation initiation codon within the US17 ORF, and another that is internal to the US17 ORF but in the opposite orientation. We cannot discount the possibility that the ΔUS17 phenotypes trace at least in part to effects on US16 or other proteins expressed from the US17 locus.

The construct was verified by viral genome restriction digestion and sequencing of PCR amplimers that span a region from 100 bp upstream to 100 bp downstream of the US17 ORF. One-step and multi-step growth analysis of ΔUS17 was performed by infecting low passage HFF at MOI of 3.0 or 0.01. Cell culture supernatants were sampled every 24 to 48 h and analyzed in triplicate by limiting dilution plaque assays. From 24 to 96 hpi (high MOI, one-step) or 2 to 11 dpi (low MOI, multi-step) ΔUS17 grew to approximately the same titer as WT AD169, and the parental BAC pAD/Cre (Fig. 6, panels A and B). A repair virus was also created in which the US17 deletion was repaired by inserting the US17 sequence back into the mutant HCMV genome fused in frame with a c-terminal V5 epitope tag (Rev17v5). This mutant had growth characteristics similar to the deletion mutant and the parental virus. Immunoblotting for

various kinetic classes of viral proteins (Immediate early 1 and 2, and late proteins pp65 and pp28) over a 96 h time course (MOI = 3.0) revealed no difference in the expression of viral proteins between ΔUS17 and parental virus (Fig. 7).

Microarray: Experiment rationale. To further examine the biological role of US17 we performed cellular transcriptional profiling of cells infected with ΔUS17 or HCMV strain AD169. We designed the beadarray experiment to encompass both early (12 hpi) and late events (96 hpi) in the HCMV replication cycle. Analyzing cellular transcripts perturbed by ΔUS17 at these time points gave detailed information on how deletion of US17 affects biological pathways at different stages during HCMV replication. The 12 hpi time point analyzed cellular events that happen before much de novo viral protein synthesis had taken place. Importantly, this time point was before US17 production during infection. Since others have noted that US12 family members influence virion assembly, we hypothesized that US17 may also be affecting virion structure. Thus, the 12 hpi time point allowed us to discriminate events that are affected primarily by changes to virion composition/structure. The late time point, 96 hpi, allowed for the identification of any pathways or genes that are directly influenced by US17 expression. US17 is produced maximally from 72 hpi to at least 120 hpi, thus, 96 hpi coincides with both US17 expression and the development of the cytoplasmic viral assembly complex (cVAC) with the goal being to study genes directly influenced by US17 that might be important for virion assembly. Genes identified as differentially regulated in the absence of US17 (ΔUS17) at 96 hpi served as hypothesis generators for down-stream experiments to identify a molecular mechanism for US17 in human cytomegalovirus biology.

Biological conditions for infection were chosen so as to maximize detection of even subtle changes to transcription caused by deletion of US17. Cells in culture are generally asynchronous, i.e., they are all at different stages of the cell cycle. This makes detection of

phenotypes difficult as cells at different points in the cell cycle have different basal states, i.e., energetic, metabolic, homeostatic, and therefore respond differently to infection. To address this, cells for the microarray experiment were seeded 72 h pre-infection and allowed to grow to confluency. This gave the cells enough time to come to metabolic equilibrium. HCMV facilitates a G1/S block in cells that is necessary for initiation of infection (122). Cells that are infected in S phase or M phase of the cell cycle must finish and return back to G0/G1 before infection can proceed (123). Synchronizing the cell population in a quiescent state (G0/G1) by growing to confluency ensured that almost every cell that is infected in our assay began the infection cycle at the same time. The high MOI of 6.0 chosen for this experiment further ensured that every cell would become infected and minimized any "bystander" effect that could happen due to uninfected cells responding to chemokines or cytokines produced by neighboring infected cells.

The beadarray is designed so that every probe is represented an average of 30 times per well. These individual probes then get averaged together to give the final detection value i.e. expression level of the transcript. Triplicate biological replicates were used, further amplifying the statistical power of the assay. Together, the high number of technical replicates per well coupled with the biological replication meant that each transcript expression level was sampled an average of ~90 times per infection condition allowing for discrimination of even subtle changes in gene expression (~ 1.35-fold from control).

Downstream analysis / statistical modeling of the bead array data was done using a software package, BRB-ArrayTools, developed by the National Cancer Institute (NCI). We have employed a variety of software features within BRB array tools that are specifically designed for differential expression analysis of microarray data. Illumina beadarray data is directly importable into BRB-ArrayTools and can be analyzed using beadarray specific plugins e.g. lumi (124) meant to take full advantage of the unique features of the beadarray platform i.e., high

number of technical replicates per probe. Once data was imported into BRB-ArrayTools, identification of differentially expressed genes was done using Significance Analysis of Microarrays (SAM), a powerful statistical algorithm specifically designed for use in differential gene expression analysis of microarray data (118). An overview of the beadarray experiment and bioinformatics workflow is illustrated in Figure 8.

Microarray experiment: Quality control. Raw expression data for the 47,213 probes from the arrays was imported and collated into BRB-ArrayTools using a beadarray-optimized robust spline normalization (124). A pre-filter was applied to eliminate probes that showed no signal differences ($P < 0.001$) across the full set of viruses, time points, and technical replicates; signal intensities of probes for 10,672 unique transcripts were then passed along for downstream analysis.

To assess consistency across replicate arrays, we used hierarchical clustering to construct a dendrogram of the unique probes identified above (centered correlation, average linkage) (Fig. 9). Two major clades were apparent, one consisting of mock infected cells (collected at the 12 hpi time point) and the two viruses at 12 hpi, and a second consisting of the 96 hpi samples for the two viruses. The mock infected and 12 hpi specimens clustered separately from the 96 hpi specimens, and transcript profiles in all infections had no correlations with mock profiles, indicating greatly altered transcription profiles in cells infected with both ΔUS17 and AD169. All sets of experimental triplicates clustered with themselves, indicating that replicate arrays were in high agreement with each other (correlations ≥ 0.80 except for ΔUS17 at 12 hpi, which had a correlation between the replicate arrays of 0.75). At 96 hpi, mutant and AD169 profiles were highly correlated (> 0.90), indicating that most host transcripts were expressed at similar levels in infections with either virus. The dendrogram illustrates that,

while, the transcript profile of ΔUS17 was highly similar to that of AD169 there were sufficient differences to classify them as distinct entities.

To analyze overall gene transcript profiles, scatterplots were constructed for both time points for all pairwise comparisons using the 10,672 probes that passed the filtering criteria (Fig. 10, panels A and B); note that SAM-significant differentially expressed probes are indicated as either black or colored dots while non-SAM significant probes are indicated as light gray dots (described in detail below). In comparison to mock infected cells, both viruses induced numerous changes to the transcription profiles at either time point. At 12 hpi, both viruses modulated over 1,800 probes infected by ≥ 1.5-fold vs. mock (Fig. 10A). At 96 hpi, changes to the transcriptional profiles were even more pronounced. Both AD169 and ΔUS17 induced over 3,000 probes by ≥ 1.5-fold vs. mock infected cells (Fig. 10B). In contrast, there were relatively few transcriptional differences between ΔUS17 and AD169, correlating with the similarity noted on the Fig. 9 dendrogram and confirming that ΔUS17 modulated only a small percentage of transcripts relative to its parent.

Differential gene expression analysis in cells infected with AD169 vs. ΔUS17. To analyze differentially expressed transcripts more robustly, we examined the specific differences in cellular transcript profiles between AD169 and ΔUS17 infections using significance analysis of microarrays (SAM) with a stringent false discovery rate (FDR) of 0.001. SAM uses gene specific t-tests to compute an expected fold change for each transcript, dε(i). It then uses permutations of the data and compares the observed fold change, d(i) to the expected foldchange. A threshold is set by using a false discovery rate (FDR) which is the number of false positives that are statically likely in the data set. If the observed fold change is larger than the threshold set for the expected fold change the gene is considered significantly differentially regulated. Output plots of the SAM analysis are shown in Figure 11. At 12 hpi, of the 10,672

probes that passed the filtering criteria, SAM indicated that only 278 were significantly differentially expressed between the two viruses (36 up- and 242 down-regulated); at 96 hpi, 97 probes were differentially expressed (22 up- and 75 down-regulated) (Fig. 10C).

To visualize the magnitude of the significant changes between AD169 and ΔUS17, SAM significant probes were plotted as black or colored dots in the Fig. 10 scatterplots. At 12 hpi, a large number of SAM significant genes that were highly up-modulated in the AD169 vs. mock dataset were relatively attenuated in the ΔUS17 vs. mock dataset, thus resulting in the population of genes down-modulated in the ΔUS17 vs. AD169 comparison. In contrast, at 96 hpi, the genes that are down-modulated in the ΔUS17 vs. AD169 comparison are the product of an amplification of down-modulation that occurred in the AD169 infections.

ΔUS17 modulates host innate and intrinsic immune responses early after infection. The genes found by SAM analysis to be significantly differentially expressed between cells infected with AD169 and ΔUS17 were categorized using Cytoscape and the biological network gene ontology plugin (BiNGO). BINGO searches for statistically over-represented gene ontology categories among a set of genes and then maps those GO categories onto a visual network. This allows for identification of clusters of gene ontology categories that, when used in conjunction with the gene ontology biological process hierarchy, highlights major biological themes of the input list of genes. At 12 hpi, BiNGO was able to categorize 239/278 (86%) of the SAM-significant genes into 259 statistically enriched biological process gene ontology categories ($P < 1x10^{-4}$). Full lists of all gene ontology categories identified are summarized in Supplemental Table 2.

To further categorize this list of gene ontology data we utilized the orthogonal layout option within Cytoscape, this minimizes edge (the lines that connect the individual category bubbles on the network) overlap between GO categories and has the effect of grouping highly

interconnected, and thus closely related, gene ontology categories next to each other. A full visual network of all significantly enriched GO categories is illustrated in Figure 12. Enrichment scores (ES) were calculated for several clusters of highly interconnected GO categories from the 12 hpi data set by calculating the inverse log of the geometric mean of the BiNGO calculated p-values for each GO categories within the cluster. Higher enrichment scores denote a lower average p value for the cluster and indicate a higher degree of average statistical significance (Fig. 13A). The most statistically significant clusters contained GO categories related to various aspects of innate and intrinsic immunity, especially, type I interferon anti-viral responses (41 categories, ES=14.6). This cluster also contained the most significantly enriched category overall "response to virus" ($P = 2.63x10^{-40}$) which contained 40/239 (17%) of the SAM-significant genes differentially modulated at 12 hpi, genes in this category are associated with sensing and responding to viral infections and include many interferon stimulated genes. Also noted were highly enriched clusters of GO categories related to regulation of various immune system processes such as leukocyte migration, production of type I interferon, regulation and production of cytokines, and regulation of Nf-κB (67 categories, ES=8.1), and apoptosis or regulation of apoptotic molecular function (32 categories ES=7.2). Two less significant clusters of GO categories were also identified and contained GO categories related to blood vessel development and angiogenesis (13 categories, ES:6.0), and metabolism (32 categories, ES=5.7). Together, genes involved in these five biological themes comprised 174 of the 239 differentially expressed genes categorized by BiNGO at 12 hpi. The other 65 genes that were SAM significant at 12 hpi, and that had gene ontology biological process information available, showed no relationship to anything in the gene ontology hierarchy that passed our threshold of significance and thus were not considered for further analysis.

Venn diagrams were constructed to highlight relationships of the individual genes in each of the five major biological process themes identified above. Of the 216 genes classified

by BiNGO, 131 of them fell under the three most significant biological themes of innate and intrinsic immunity, regulation of immune processes, and apoptosis (Fig. 13B). Genes in these categories showed a large degree of overlap with each other with few unique genes in each theme, with the exception of innate and intrinsic immunity which had 44 genes that were not classified in any other category. We next compared the two less significant biological themes of metabolism and blood vessel development. Again, transcripts in these categories were found to have a high degree of overlap with GO categories related to the more statistically significant immune response and apoptosis GO clusters (Fig. 13B). Taken together, the high degree of overlap between the five identified themes indicates that the most significant of them, innate and intrinsic immunity, represents the major biological theme of the genes differentially expressed at 12 hpi.

To put these results into the broader context of host immune responses during HCMV infection, we compared expression of the 131 innate and intrinsic immunity related SAM significant transcripts differentially regulated by ΔUS17 with that of mock infected cells and visualized them by overlaying the genes on the Figure 10 scatterplots. The subset of immune/apoptosis related transcripts identified above was readily apparent, showing a high degree of up-modulation in the AD169 vs. Mock pair but a relative attenuation of up-modulation in the ΔUS17 vs. Mock pair wise comparison. The net result was an overall down-modulation of these transcripts between ΔUS17 and AD169 (Fig. 10A gold dots). Of the 131 innate and intrinsic immunity related transcripts, 123 were differentially down-modulated in this fashion by ΔUS17 compared to AD169, with 54 of those transcripts being ≥ 2-fold down-regulated. Many of the most highly down-regulated genes encode either interferon stimulated genes or soluble factors, namely cc and cxc chemokines and cytokines. These transcripts grouped into two highly significant gene ontology categories identified above; “Type I interferon mediated signaling” ($p= 6.22 \times 10^{-32}$, 21 probes) and “Inflammatory Response” ($p= 3.27 \times 10^{-7}$, 8 probes).

Expression levels of genes in these two categories are illustrated in Figure 14. Complete lists of all SAM-significant genes at 12 hpi and 96 hpi, and transcripts common to both time points are provided in Supplementary Table 1.

To further confirm the phenotype observed using the microarray, we employed a custom qRT-PCR array that targets six innate and intrinsic immune response transcripts that showed a high degree of down-modulation compared to AD169 at 12 hpi. We compared the parental virus pAD/cre, a BAC version of AD169 which contains no deletion of primary sequence but does contain a small 32 bp lox scar between the US28 and US29 ORFs, two independently derived ΔUS17 mutant viruses (ΔUS17 and 2ΔUS17), and a US17 deletion repair virus (US17cV5). The two independent ΔUS17 viruses showed the same down-modulation as was observed on the microarray (Fig.15). Additionally, the repair virus restored transcript expression to parental levels, indicating that deletion of the US17 locus had a specific effect on expression of immune genes. Overall, these changes in gene expression at 12 hpi, a time that precedes de novo expression of most HCMV genes, suggest changes in the way ΔUS17 virions are sensed by the host cell.

Gene ontology analysis at 96 hpi. At 96 hpi, BiNGO categorized 86 of the 98 SAM significant genes into 76 significantly enriched GO biological process categories ($P < 1x10^{-4}$). As evident in the scatterplots (Fig. 10 A and B), differences between ΔUS17 and AD169 were generally smaller than at 12 hpi. Fourteen of the over-represented biological process categories related to type I interferon, cytokine, or various other aspects of immune responses and another five categories related to apoptosis (Supplementary Table 2). Together, these categories contained 43 differentially regulated transcripts, 22 of which were identified by SAM analysis as being differentially expressed between AD169 and ΔUS17 at both 12 hpi and 96 hpi (Fig. 10C). Interestingly, for most of these genes, although the magnitude change relative to mock

decreased from 12 to 96 hpi, the directions of the transcriptional changes were consistent at both times, with ΔUS17 blunting induction of certain immune response transcripts (predominantly interferon responsive genes) while amplifying the suppression of other transcripts (predominantly genes involved in tissue development). In sum, ΔUS17 produces pronounced changes to host immune transcripts at 12 hpi that persist to at least 96 hpi.

Several ER stress and unfolded protein response transcripts were differentially regulated at 96 hpi but not at 12 hpi. This included a number of heat-shock 60 kDa (HSP60) proteins, as well as transcripts for proteins involved in ER stress and the ER associated degradation (ERAD) pathways. Positive and negative effects were seen among transcripts associated with these genes (Fig. 14). At least one of these genes (HSPA5 or Bip) is important for the biogenesis and function of the HCMV cytoplasmic virion assembly complex (cVAC) (110,125). US17 shows its highest levels of expression from 96 to 120 hpi, thus, transcripts modulated by ΔUS17 at late times are probably a direct effect of the mutation rather than the indirect effects seen at 12 hpi.

Discussion

US17 indirectly modulates host innate and intrinsic immune responses. As for other infectious agents, modulation of immune responses is a fundamentally important aspect of HCMV biology. The process of HCMV host cell immunomodulation begins at the very earliest stages of viral attachment to the cell and is highly dependent on the structural components of the virion, i.e., envelope glycoproteins such as gB and gH, and tegument proteins such as pp65 (114,126-128) reviewed in (9). We found that deletion of US17 had little impact on production of infectious viral particles in fibroblasts, but nevertheless exerted a tangible influence over viral replication. ΔUS17 markedly blunted the host cell anti-viral response at a very early time point (12 h) after infection. Many interferon stimulated transcripts and transcripts encoding for pro-inflammatory chemokines and cytokines were down-modulated by 3- to 5-fold when compared to the parental virus. These changes to immune sensing of the host cell at 12 hpi happened in the absence of US17 expression, thus we conclude that virions produced by ΔUS17 infected cells differ in their composition from those produced by parental virus.

A role for US17 mediated manipulation of ER stress responses late in infection. In contrast to the modulation of immune responses at 12 hpi, other effects were seen at 96 hpi, a time that corresponds with both high expression of US17 and the formation of the cVAC (96). Specifically, expression of some ER stress response and chaperone transcripts were significantly altered by ΔUS17. By unknown mechanisms, HCMV modulates various pathways and genes involved in ER stress and the unfolded protein response (106,108). One such gene, HSPA5 (GRP78/BIP), which was up-regulated 1.6-fold by ΔUS17, is important for formation of the cVAC and production of infectious virions (110,112,125). Several other important regulators of ER stress were also modulated, including DDIT3 (also known as CHOP) (2.11-fold increase) and CHAC1 (1.6-fold increase), both of which are known to promote apoptosis during the ER stress response (129-131). Relative to mock-infected cells, ΔUS17 and its parent altered

regulation of most of these transcripts in opposite directions. This is in sharp contrast to the sets of immune transcripts that at 12 hpi were modulated by ΔUS17 and its parent in the same direction relative to mock-infected cells.

The modulation of gene expression by US17 at later stages of infection provides insights into a potential mechanism of action for US17 and offers cellular targets that could be studied in this context. We note that US12 family members share sequence similarity with the trans-membrane bax inhibitor-1 (TMBIM) family of conserved eukaryotic anti-apoptotic seven transmembrane proteins (71). These proteins localize to membranes of various cellular organelles where they act as rheostats that modulate apoptotic and ER stress signaling by influencing cellular calcium levels (80-84). Interestingly, over expression of Bax inhibitor-1, showed lower levels of expression of both BIP and CHOP in response to the ER stress inducers thapsigargin and tunicamycin (132). This is directly opposite to the phenotypes observed here where deletion of US17 exhibited higher expression of both BIP and CHOP in response to HCMV infection. Taken together, it is possible that US17 is a bax inhibitor-1 ortholog that shapes virion composition by modulating levels of ER stress response and apoptosis genes involved in regulation of protein folding, trafficking, and cVAC function.

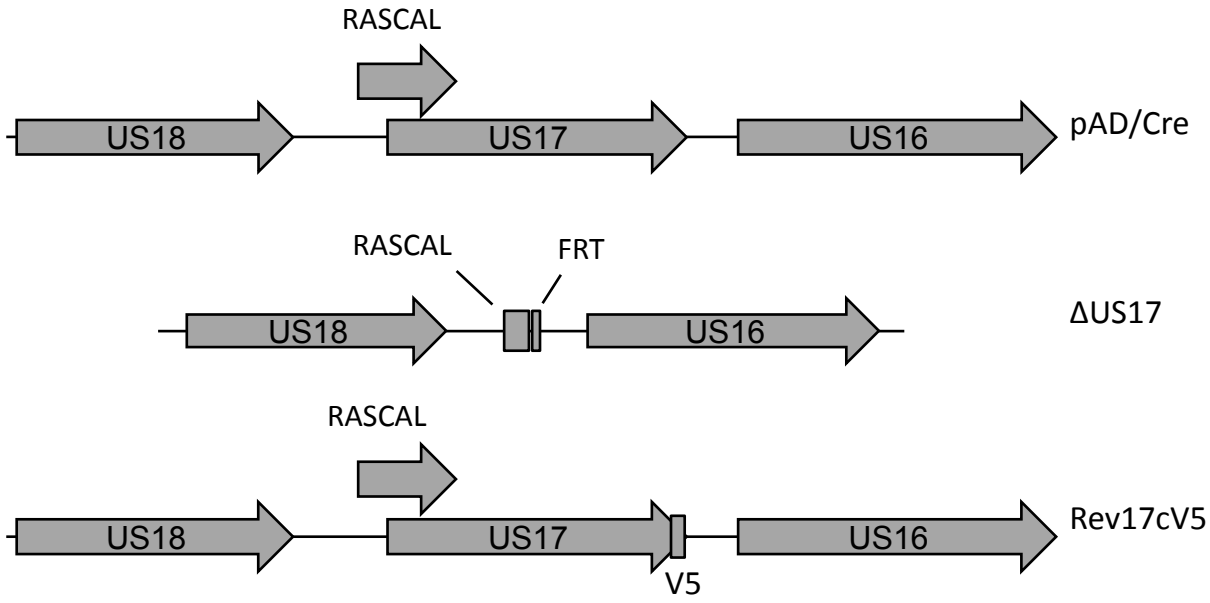

Figure 5. **Schematic detailing recombinant viruses used in this study.** Bacterial artificial chromosome recombineering was used to generate a virus deleted in frame for US17 leaving only a 32 bp FRT scar (ΔUS17). The deletion mutant was repaired by insertion of the wild type US17 sequence in place of the FRT scar with an additional C-terminal V5 small epitope tag (Rev17cV5).

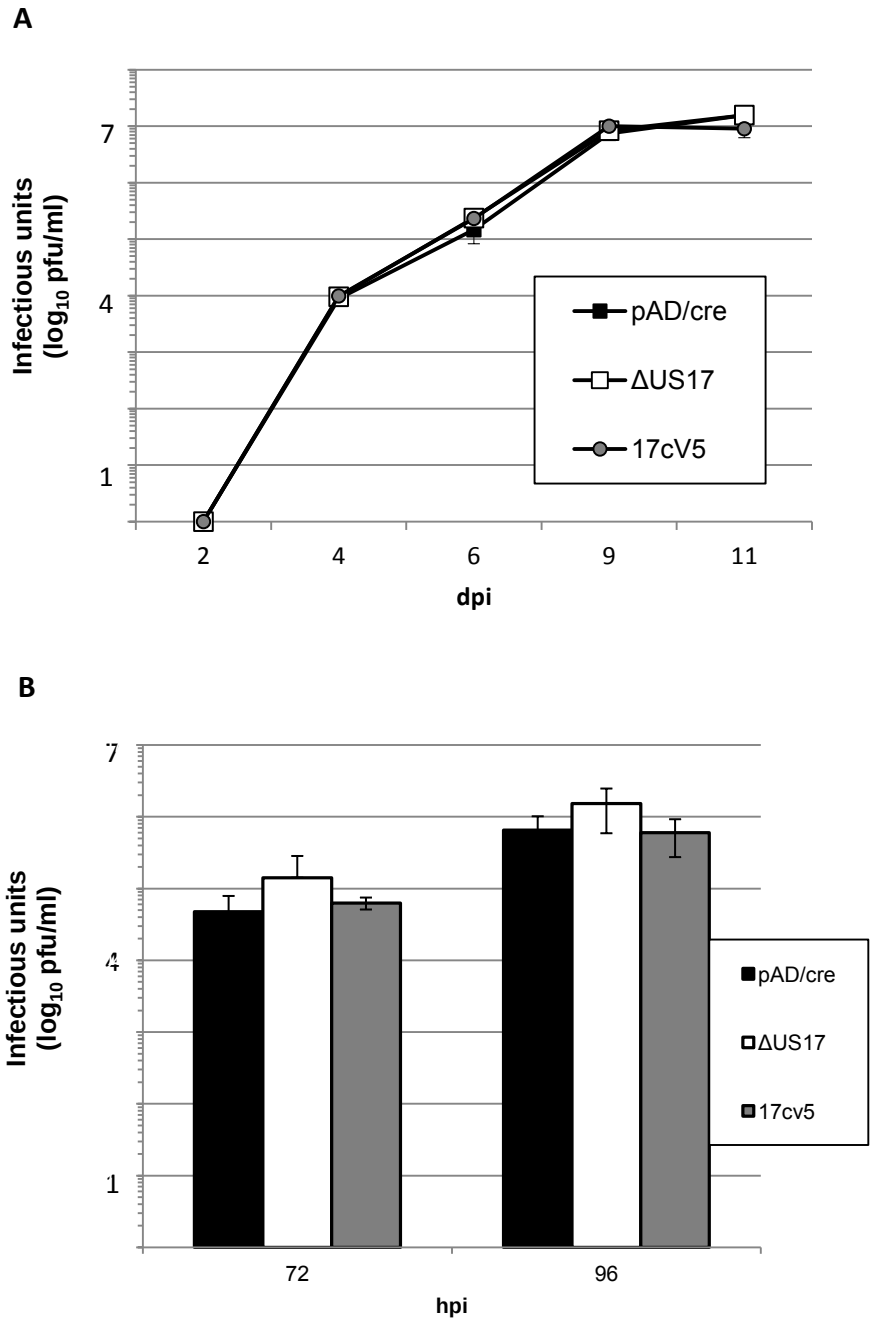

Figure 6. **Deletion of US17 does not significantly affect production of infectious virus in fibroblasts.** (A) Multistep (MOI=0.1) and (B) Single step (MOI=3.0) growth curves comparing production of infectious virus using the parental virus pAD/Cre, the US17 deletion mutant (ΔUS17), and the repair virus Rev.cV5.

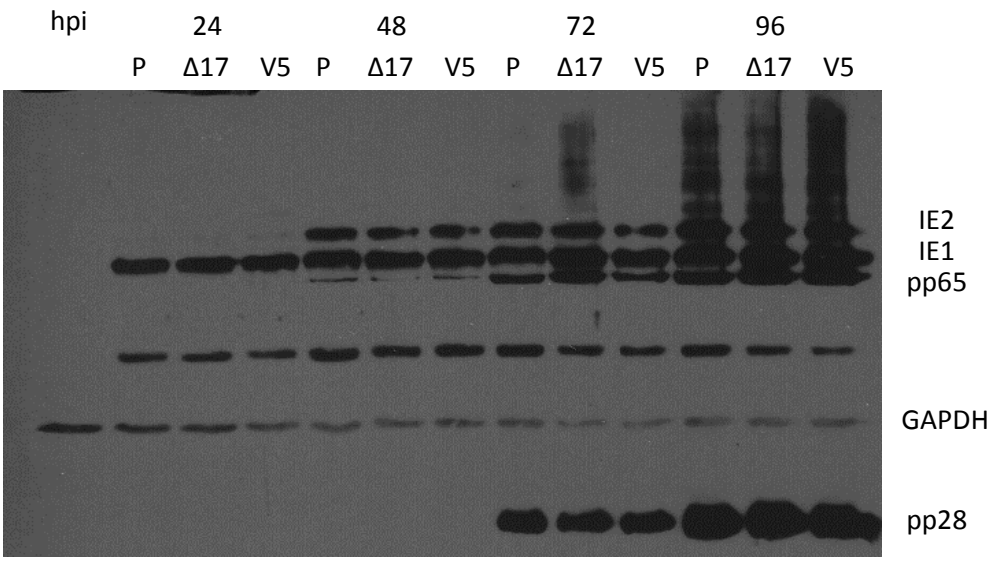

Figure 7. **Deletion of US17 does not alter production of viral proteins.** Immunoblot of cellular lysates from HFF infected with either pAD/Cre (P), ΔUS17 (Δ17) or the repair virus 17cV5 (V5) at MOI = 3.0 for 24 to 96 hpi.

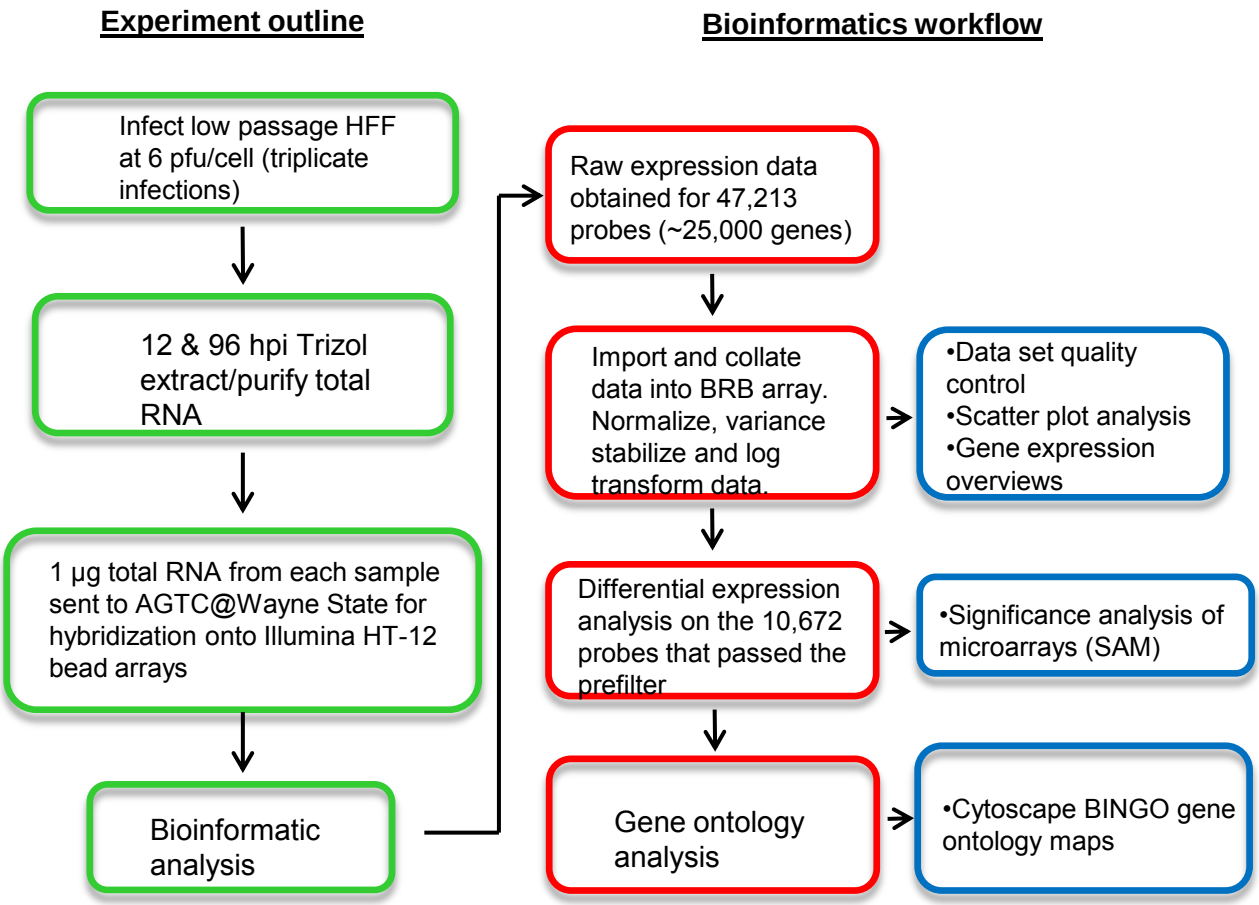

Figure 8. **Beadarray experiment overview and bio-informatics workflow.**

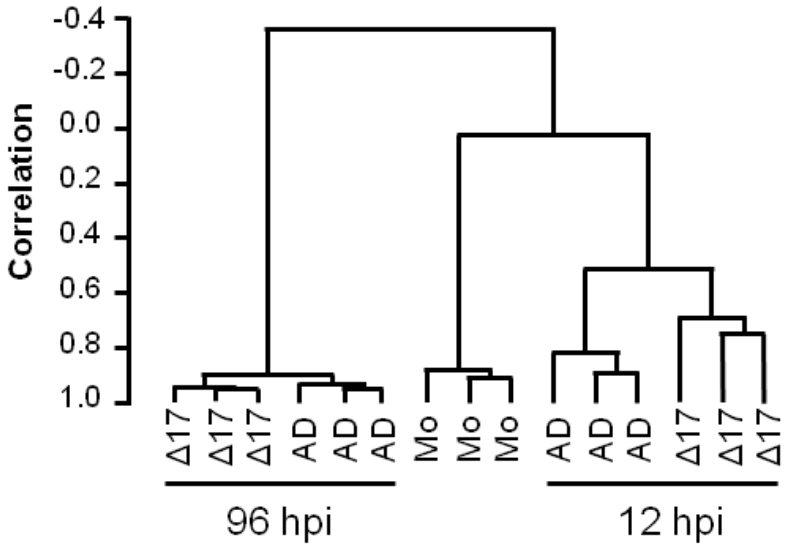

Figure 9. **ΔUS17 alters small sets of host transcripts at both 12 and 96 hpi.** Dendrograms showing the relationships of cellular transcript profiles generated by Illumina HT-12 beadarray analysis. Three biological replicates were analyzed for each virus and are as follows: AD = AD169, Δ17 = ΔUS17 and Mo = Mock infected. Correlation scores closer to 1 denote a higher degree of similarity between two clades.

Figure 10. **Transcripts modulated by ΔUS17 at 12 and 96 hpi found significant by SAM.** A and B: Pair-wise scatterplot analysis of the 10,672 probes that passed the initial pre-screen filter. Colored dots indicate SAM-significant differentially regulated gene sets between ΔUS17 and AD169 (FDR = 0.001) as follows: Black: non-immune SAM significant genes, yellow: SAM significant innate and intrinsic immune related genes differentially expressed at 12 hpi, light blue: SAM significant innate and intrinsic immune related genes differentially expressed at 96 hpi. Black lines represent ≥1.5 fold change in either direction. C: Venn diagrams of total SAM significant transcripts and immune related SAM significant transcripts at 12 and 96 hpi.

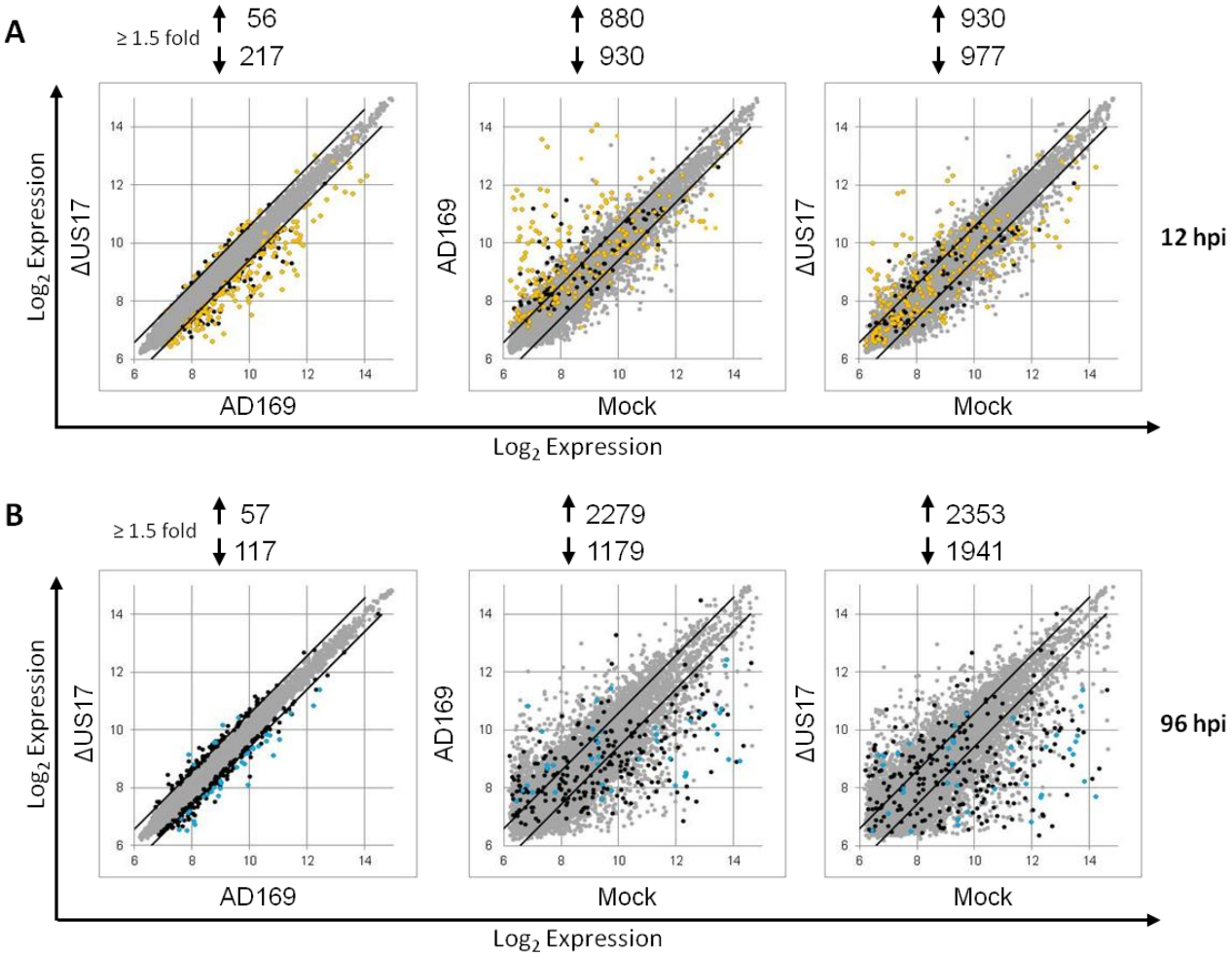
A
≥ 1.5 fold
56
217
880
930
930
977
ΔUS17
AD169
ΔUS17
AD169
Mock
Mock
Log2 Expression
Log2 Expression
12 hpi
B
≥ 1.5 fold
57
117
2279
1179
2353
1941
ΔUS17
AD169
ΔUS17
AD169
Mock
Mock
Log2 Expression
Log2 Expression
96 hpi

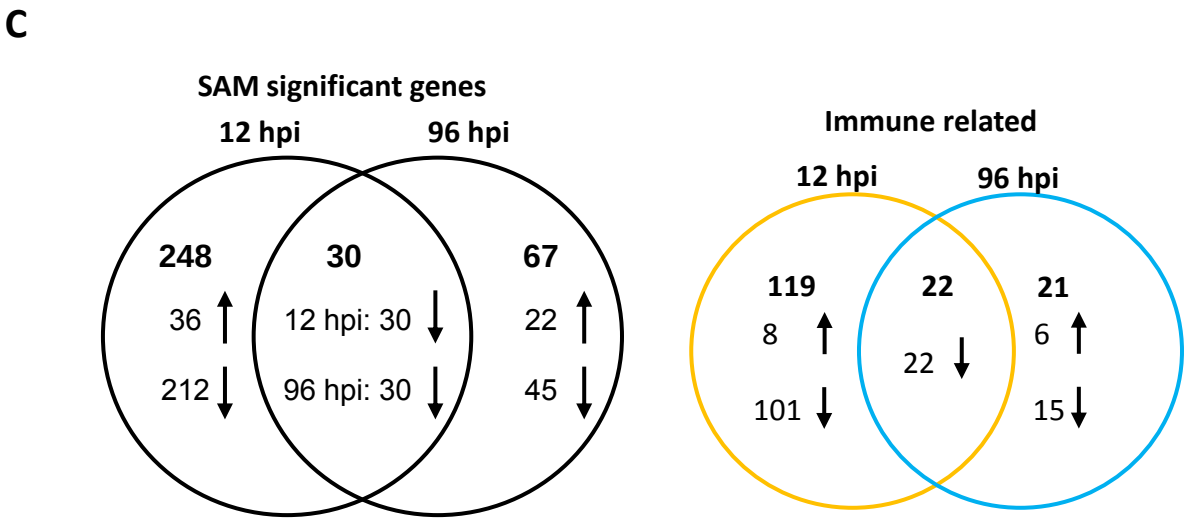
C
SAM significant genes
12 hpi
96 hpi
248
36
212
30
12 hpi: 30
96 hpi: 30
67
22
45
Immune related
12 hpi
96 hpi
119
8
101
22
22
21
6
15

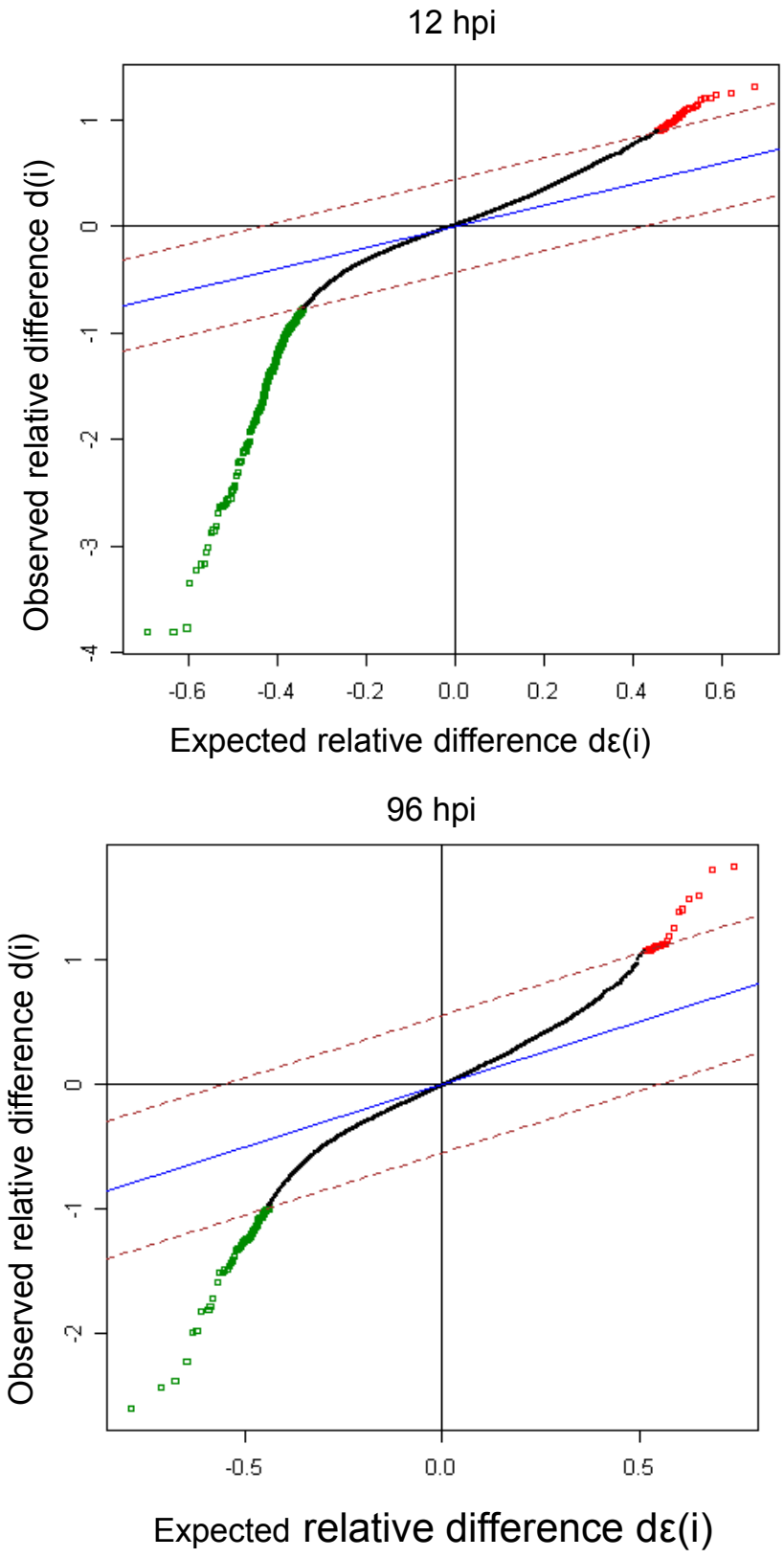

Figure 11. **SAM plots of genes differentially regulated by ΔUS17 compared to AD169.** The threshold, representing a FDR of 0.001 is the dashed red line. Genes significantly up-regulated by ΔUS17 vs. parental virus are shown as red dots while down-regulated genes are shown as green dots.

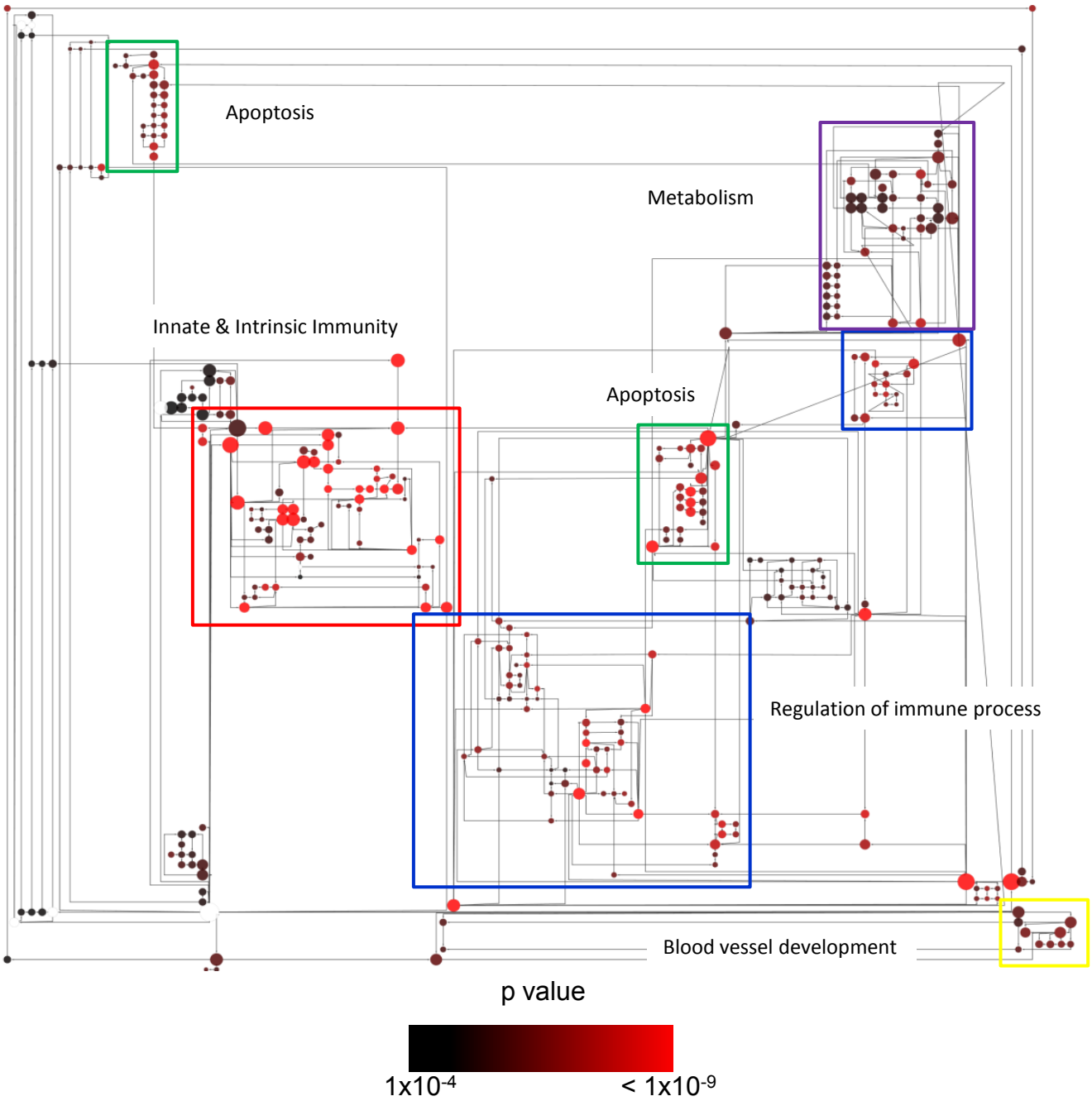

Figure 12. **Cytoscape gene ontology maps of genes significantly regulated by ΔUS17 compared to parental at 12 hpi.** Lists of SAM significant genes were imported into cytoscape using the BiNGO plugin. Gene ontology biological process maps were generated using a p value cutoff of 0.0001. Categories are color coded based on p value with black being the least significant and red representing the most significant. Maps were organized using an orthogonal layout which clustered closely connected GO categories next to each other. Colored boxes represent the five biological themes identified.

A

Group	GO biological theme	GO categories (n=259)	Genes (n=239)	Enrichment score
A	Innate immunity & Interferon production	41	131	14.6
B	Regulation of immune response	67	93	8.1
C	Apoptosis	32	86	7.2
D	Blood vessel development/ angiogenesis	13	44	6.0
E	Metabolism	32	71	5.7

B

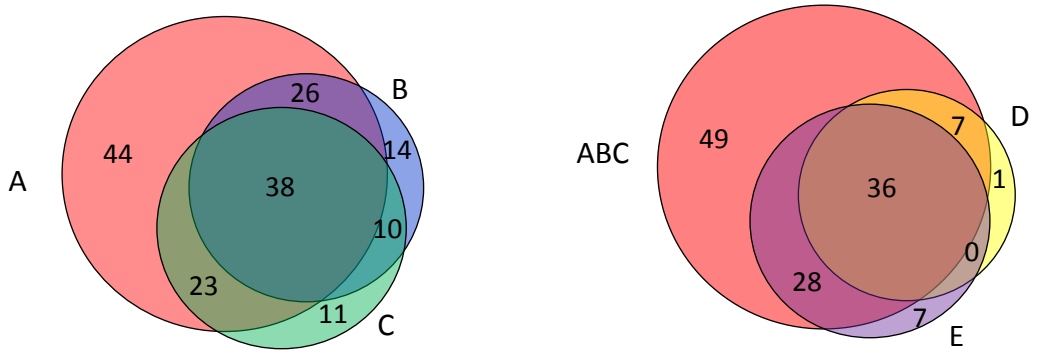

Figure 13. **Gene ontology analysis of SAM significant transcripts.** (B) Table outlining the five biological themes identified. Listed are the numbers of individual gene ontology categories for each theme out of the 259 total GO categories identified as statistically significant ($P < 0.0001$). Also listed are numbers of SAM significant transcripts in each theme out of the 239 that could be categorized into a gene ontology biological process category. The enrichment score denotes the average level of significance of all of the GO categories in a particular theme. Higher enrichment scores indicate a more significant, mean log transformed p value for that theme. (A) Venn diagrams detailing numbers of differentially modulated SAM significant transcripts from the ΔUS17 vs. AD169 12 hpi comparison that grouped into the five most highly significant biological categories identified by BiNGO gene ontology biological process clustering. The left Venn diagram is a comparison of transcripts that grouped into either of the three most significant gene ontology themes of innate immunity and interferon production, regulation of immune response, or apoptosis. The right Venn diagram is a comparison of transcripts that grouped into either of the first three themes against the two minor identified gene ontology themes of blood vessel development and metabolism.

Figure 5.

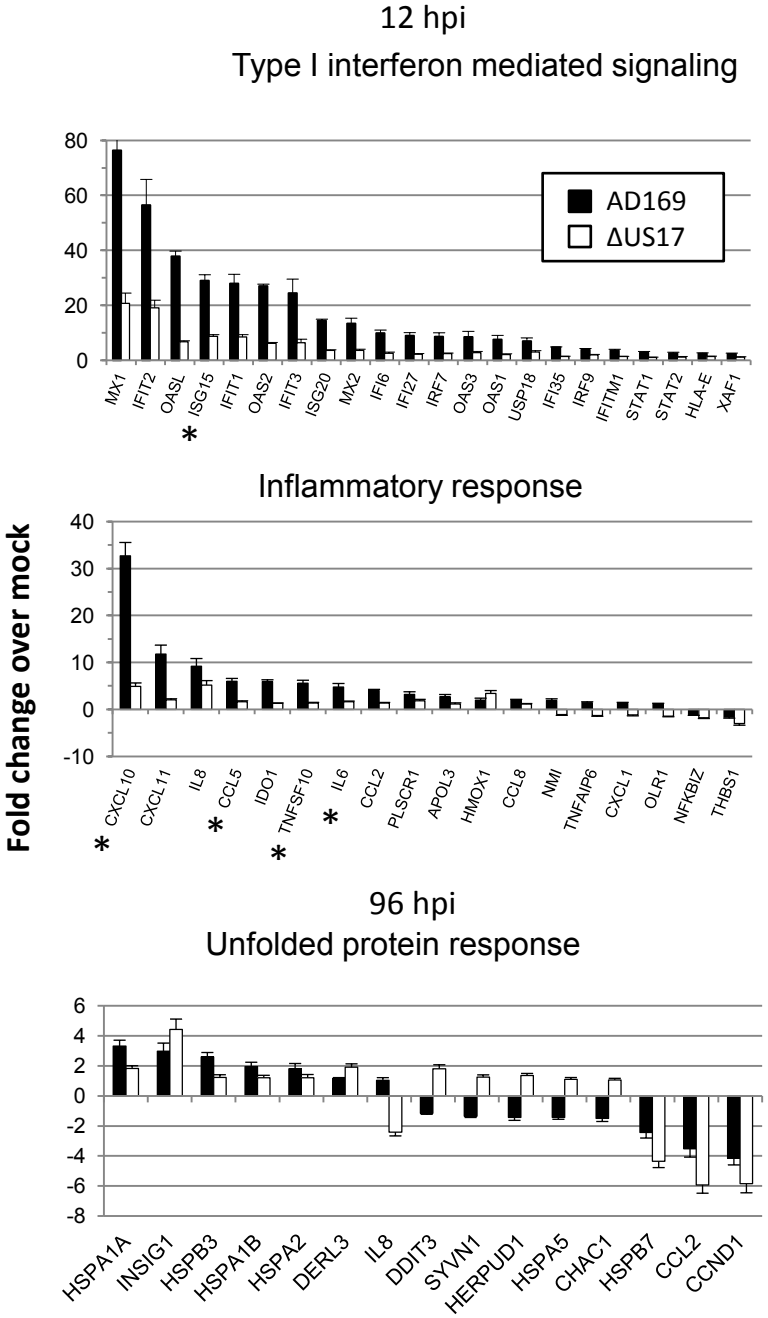

Figure 14. **Transcript expression profiles for several GO categories highly significantly enriched at either 12 or 96.** 12 hpi categories include "Type I interferon mediated signaling" ($p = 6.22 \times 10^{-32}$) which includes mainly anti-viral interferon stimulated transcripts and "Inflammatory response" ($p = 3.27 \times 10^{-7}$) comprised of mainly pro-inflammatory cytokine and chemokine transcripts. At 96 hpi one GO category "Response to unfolded protein" is highlighted ($p = 2.53 \times 10^{-8}$). Asterisks denote genes validated by Taqman qRT-PCR.

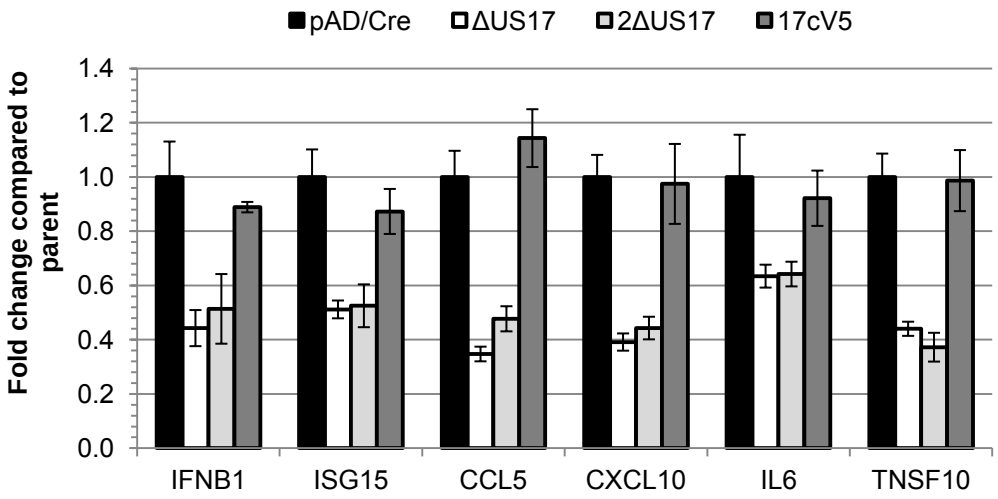

Figure 15. **qRT-PCR verification of beadarray identified transcripts.** Low passage HFF were infected with either the parental BAC virus (pAD/Cre) , either of two independently generated ΔUS17 virus, or the US17 deletion repair virus (17cV5) for 12 h at moi = 3.0. Taqman qRT-PCR was performed with primers specific for six different genes that were highly differentially regulated by ΔUS17 at 12 hpi. Shown are the averages of biological replicates, three for pAD/cre, two for ΔUS17, three for 2ΔUS17, and one for 17cV5. Three technical replicates were performed for experiment. Error bars indicating one standard deviation.

Chapter Three

Role of US12 family proteins in regulating virion assembly.

Introduction

The HCMV virion has a highly complex structure. Analysis of purified virion preparations has indicated that there may be as many as 70 different viral proteins incorporated to form a mature infectious virion (94,95). We have previously shown, in chapter one of this work, that a recombinant HCMV deleted for one member of the US12 protein family, ΔUS17, elicited a blunted immune response from host cells at early times after infection (12 hpi). This time was before US17 expression during infection, leading us to hypothesize that US17 may be influencing virion composition.

The viral mediators of HCMV virion assembly are presently not well understood. Various proteins in the US12 family, e.g. US16 and US18 (described previously), have been implicated in modulating virion protein structure (74,75). These hypotheses have been driven largely by inferring changes to virion composition from observations of growth phenotypes using deletion mutants in various cell types. To date, no groups have elucidated any particular functions associated with US12 family members nor have any specific changes to virion structure been shown in the absence of US12 family member expression.

Thus, to directly study the effects of US17 on virion structure, we gradient purified virions from ΔUS17 infected cell culture supernatants to compare protein composition, infectivity, and levels of incorporated viral genomes to that of parental virions. We discovered that ΔUS17 virions differ from parental in a number of key ways. First, ΔUS17 virions had reduced amounts of the viral glycoprotein, gH, incorporated into their structure. Second, fibroblasts infected with ΔUS17 produced 3-fold more non-infectious genome-containing virions than parental virus.

Third, when inoculated at equal MOIs ΔUS17 virions delivered a 3-fold larger amount of the tegument protein pp65 compared to parental virions.

US12 family members share some homology to the TMBIM family of eukaryotic ER stress and anti-apoptotic proteins (133). The importance of ER stress pathways in virion maturation, assembly complex formation and function (described in the general introduction of this work), coupled with the sequence similarity of US12 family members to the TMBIM family of ER stress and UPR related proteins and indicates that US12 proteins may indeed be playing a role in modulating virion composition possibly by affecting pathways involved in protein folding or protein trafficking of viral tegument and glycoproteins from the ER to the cVAC.

Materials and methods

Gradient purification of viral particles. Supernatants were harvested 10 dpi from low passage (p 10) HFF infected at an MOI of 0.01 with the parental strain pAD/cre, ΔUS17, or the US17 deletion repair virus US17cV5. Supernatants were clarified by centrifugation at 3,000 RPM for 15 m. Viral particles were subsequently concentrated by centrifugation through a cushion of 20% sorbitol in TN buffer (50 mMol Tris pH 7.4, 100 mMol NaCl) at 60,000 xg for 1 h using a Beckman SW 41 Ti rotor. Virion pellets were re-suspended in a small volume of TNE (50 mMol Tris pH 7.4, 100 mMol NaCl, 10 mMol EDTA) and layered over a 10 – 50% linear Nycodenz gradient prepared in TNE (Axis-shield, Oslo, Norway). Gradients were centrifuged at 110,000 xg for 2 h in a Beckman SW 41 Ti rotor and subsequently top fractionated into 1 ml aliquots. To dialyze each fraction into PBS, Ultrafiltration of concentrated virus was carried out with an Ambicon 10 kDa cutoff filter (EMD-millipore). Samples were first diluted with an additional 1 ml PBS and centrifuged at 3,000 rpm for 30 – 45 m to concentrate to 100 µl. An additional 2 ml of PBS was added and samples were centrifuged at 3,000 rpm for an additional 30 – 45 minutes until a final volume of 100 µl was obtained.

Immunofluorescent microscopy. HFF were seeded 72 hours pre-infection onto gelatin coated 8 well chamber slides (Thermo Scientific, Rochester, NY) and infected at an MOI of 3.0 with the indicated virus. 2 hpi cells were fixed in 4% para-formaldehyde for 10 m at room temperature and quenched in 50 mm NH_4Cl for 10 min. Cells were permeabilized in a blocking buffer consisting of 10% normal goat serum, 5% glycine in PBS and 0.2% triton x-100. Antibody staining was conducted using appropriately diluted primary anti-body against pp65 (Fitzgerald Industries Acton, MA) and Alexa-fluor 488 secondary antibody (Molecular Probes/Life Technologies Grand Island, NY). Images were captured using a Nikon Eclipse e800 microscope and total fluorescent signal was measured using Image J software. Three random

images were taken for each of two biological experiments. Images were background corrected by measuring the average fluorescent intensity of an area that contained no pp65 signal. Thresholds were set to measure only pp65 signal in the nucleus and the punctuate staining in the cytoplasm of each cell. Total fluorescent intensity of the thresholded image was divided by the number of pp65 positive nuclei to obtain the final pp65 signal intensity value.

.

Results

ΔUS17 induces changes in virion protein composition. Changes in cellular gene expression at 12 hpi were unexpected (presented in Chapter 1 of this work), given that US17 is a late gene whose expression is dependent on viral DNA synthesis, and is not detectably expressed in infected cells until at least 48 hpi. We hypothesized that changes in transcription of cellular interferon and innate immune genes at 12 hpi were the product of changes in virion protein composition caused by the absence of US17. In order to directly analyze the protein composition of ΔUS17, parental, or the US17 deletion repair virus US17cV5 virions, we subjected infected cell-culture supernatants (MOI=0.01, 10 dpi) to density gradient centrifugation through a 10-50% linear Nycodenz gradient. This separated viral particles based on buoyant density and allowed for discrimination of any physical differences in the particles produced by ΔUS17 compared to those produced by the parental virus. Nycodenz offers a non-ionic, non-osmotic alternative for gradient purification of viral particles. Traditional linear gradients of sucrose or potassium tartrate rely on high concentrations of salt which inactivate many of the infectious particles thus making down-stream analysis difficult. Further, Nycodenz gradients have been previously used to purify the various particle types from HCMV cell culture supernatants, e.g., NIEPs, dense bodies (95).

Initial observations of the gradients revealed a thick milky-white band that concentrated between fractions 4 and 7 which presumably contained the majority of the viral particles (Fig. 16). The band was located at approximately the same location in gradients of the parental virus, ΔUS17, and the repair virus indicating that the particles produced by ΔUS17 were of a similar density to parental virions. The gradients were top fractionated into 10-1 ml aliquots (indicated as red lines in Fig. 16) dialyzed into PBS using an Ambicon ultra-filtration unit with a 10 kDa cutoff, and DNase treated to remove any non-encapsidated viral DNA. To determine

the relative amount of viral DNA present in each fraction, viral genomes were extracted and subjected to qPCR using a set of primers specific for the HCMV UL83 ORF. As expected, fractions 4 – 7 contained 92 – 98 % of the viral DNA in the entire gradient for each virus coinciding with the observed milky band. Fraction 5 was especially enriched for viral genomes and contained approximately 70% of the genetic content of the entire gradient (Fig. 17). Fraction 5 showed similar levels of viral DNA for all three viruses in. However, differences in amounts of viral genomes were detected in fractions 4, and 6. ΔUS17 displayed a lower level of viral genomes present in fraction 4 while we observed lower levels of parental virus genomes in fraction 7. Interpretation of these results is complicated and it is unclear if these differences are due to particles of different densities being produced by ΔUS17 or do to loss of material during the concentration, manual fractionation of the gradients, or ultrafiltration / dialysis. Given this limitation we have preformed down-stream analysis using a variety of techniques, i.e., plaque assay and immunoblotting, which allowed us to normalize based on the numbers of particles present in each sample.

To analyze levels of specific viral proteins we compared the protein profiles of gradient-purified virions present in fraction 5 by silver staining and immunoblotting for three tegument proteins (pp65/pUL83, pp28/pUL99, and the large tegument protein/pUL48) as well as two virion surface glycoproteins (gB/pUL55, and gH/pUL75). Differences in relative abundance were noted for several protein bands on the silver stain, indicating that virions produced by ΔUS17 differ from those produced by the parental virus (Fig. 18A). These changes were not attributable to an overall difference in the amount of protein loaded as the majority of the bands observed were relatively equal in abundance. This indicates that virions produced by ΔUS17 differ from the parental virus with respect to their protein composition. Densitometric analysis of the immunblot revealed no gross changes for any of the tegument proteins, pp65, pp28, or pUL48. However, there was a ~2.8 fold decrease in ΔUS17 virion levels of the envelope

glycoprotein, gH, while gB levels were unchanged (Fig. 18B). Virions from the repair virus displayed levels of gH that were equal to parental indicating a specific effect of deletion of the US17 locus. Glycoprotein H (gH) has a linear length of 742 amino acids and has a predicated size of ~75 kDa, thus, it is the right size to correspond with the ~75 kDa protein band that showed a reduced level in the silver stain (Fig. 18A middle arrow). These changes to virion protein content indicate that although equal levels of infectious virions are produced, some aspects of virion assembly are altered in the absence of the US17 coding region. Furthermore these changes to virion compositions elicited by deletion of the US17 locus are specific to what appears to be a small subset of viral proteins.

ΔUS17 alters the genomes-to-pfu ratio of infected cells. Having shown that growth curves in HFF of viruses deleted for the US17 coding region are indistinguishable from the parental virus (Fig. 6A and B), we hypothesized that virions produced by ΔUS17 differ from the parental virus with respect to the genomes-to-pfu ratio. We first analyzed gradient fractions by plaque assay to measure the infectious titer of each virus. We specifically focused on fraction 4 through 7 because, as previously stated, these four fractions contained between 92 and 98% of the total genetic and infectious content of the gradients. ΔUS17 contained lower levels of infectivity in fractions 4 and 5 (10-fold and 3-fold decreased respectively) but approximately equal levels compared to parental in fractions 6 and 7 (0.77 and 0.95 respectively). In contrast, the C-terminal v5 repair virus contained approximately equal titers compared to the parental virus in fractions 4, 5, and 7 but had higher levels of infectivity in fraction 6 (Fig. 19A).

We analyzed the genetic content of each fraction using qPCR. ΔUS17 contained relatively more DNase I protected genomes in fraction 5 – 7 even though the levels of infectivity were slightly lower than parental in 5 and 6 and equal in fraction 7 (Fig. 19B). The repair virus Rev. 17cV5 also contained higher levels of genomes than parental in fractions 5 and 6 but, in

contrast to ΔUS17, this increase in genetic content corresponded to higher levels of infectious virus compared to the parental virus. Taken together, when genome-to-pfu ratios were calculated, ΔUS17 displayed over a 3 : 1 ratio of non-infectious viral particles compared to parental in fractions 5, 6, and 7 (3.65, 3.55, and 4.12 to 1 respectively) while the repair virus had ratios that were almost equal to the parent virus (1.65, 1.49, and 2.37 to 1 respectively) (Fig. 19C). This indicates that ΔUS17 is producing more non-infectious genome-containing viral particles than either parental virus or the US17cV5 repair virus. These virions cannot be accounted for by limiting dilution plaque assay but they are of a density that is similar to that of the bulk of the infectious particles produced as they localize to the same fraction on the gradient.

The previous experiment used a low MOI and relatively long time course of infection. Thus to elucidate the time frame after infection when these non-infectious particles are produced we repeated the experiment at a high multiplicity of infection (MOI=3.0) and shorter time course of 24 to 96 h. At 72 and 96 hpi, times when equal numbers of infectious virions were produced by both viruses (Fig. 20A), ΔUS17 produced 3.7- and 3.8-fold more genome-containing viral particles (Fig. 20B). To obtain the genomes-to-pfu ratio, fold changes in levels of DNase protected genomes were divided by fold changes in infectious titer between ΔUS17 and pAD/Cre. ΔUS17 produced 3.4 genome-containing non-infectious particles for every such particle produced by the parental virus at 72 hpi ($p=0.001$) and a similar increase at 96 hpi (3.3:1, $p=0.0003$) (Fig. 20C). The repair virus had ratios similar to those of the parental virus (pAD/Cre).

The elevated genomes-to-pfu ratio of ΔUS17 was consistent over multiple experiments using a variety of biological conditions, i.e., MOIs ranging from 0.001 to 6.0 with time courses ranging from 3 dpi to 14 dpi. Although we did see changes in the numbers of infectious units

produced by ΔUS17 in the gradient purified fractions we attribute this to a loss of particles during the purification process. We have generated multiple stocks of both pAD/Cre and ΔUS17, and have consistently detected higher genomes-to-pfu ratios for ΔUS17 while levels of infectious virus were always within 1- to 3-fold of parental. Thus, ΔUS17 produces a larger quantity of non-infectious genome-containing particles while producing the same number of infectious particles as the parental virus.

Effects of ΔUS17 altered virions on the initial stages of viral infection. We studied the effects of this altered genomes-to-pfu ratio on the initial stages of viral infection, specifically, delivery of tegument proteins to infected cells. We hypothesized that the increase in non-infectious viral particles delivered by ΔU17 at a given multiplicity of infection would result in increased input levels of tegument proteins. We focused on tegument protein pp65, as it is a major constituent of the virion structure and is delivered in sufficient quantities to infected cells to allow for visualization of input protein immediately after infection. Also, pp65 directly down-regulates expression of several interferon genes identified as being differentially regulated by ΔUS17 at 12 hpi. Thus, if the excess of non-infectious viral particles produced by ΔUS17 could enter into and deliver higher levels of pp65 and other tegument proteins to infected cells this might explain the observed differences in immunomodulation by ΔUS17 at 12 hpi.

To directly visualize the amounts of pp65 delivered during virion entry, we employed immunofluorescence microscopy on cells infected at MOI = 3 at 2 hpi, a time when little de novo viral protein production could have taken place. In comparison with parental virus, ΔUS17 displayed a 2.6-fold ($p = 0.001$) increase in the level of intracellular pp65 delivered to each cell infected with ΔUS17. Localization of the pp65 signal was not altered in ΔU17 infected cells, with the majority of the signal residing in the nucleus and nucleoli, and small amounts of pp65 remaining as punctuate staining in the cytoplasm. Representative fluorescent images are

shown in Fig. 21A. The quantitation shown in Fig. 21B is the mean fluorescent intensity from three random fields taken from each of two biological experiments. The increase in pp65 delivered to newly infected cells corresponds well with the ~3-fold increase in non-infectious viral particles produced by ΔUS17 observed via qPCR.

Discussion. We previously demonstrated that fibroblasts infected with ΔUS17 produced virions elicited a blunted immune response from host cells at early times after infection (12 hpi) in comparison to virions of the parental virus. This phenotype was in direct contrast to other studies using recombinant HCMV deleted for the immunomodulatory tegument protein pp65, which elicited a vastly increased interferon response from host cells (113,114). We further observed that cells infected with ΔUS17 produced 3-fold more genome-containing non-infectious viral particles compared to the parental virus. When cells were infected at equal multiplicities of infection the larger number of non-infectious particles entered host cells and delivered larger amounts of the immunomodulatory tegument protein pp65. The additional pp65 and possibly other tegument proteins delivered by the excess of non-infectious viral particles produced by ΔUS17 likely explain the observed blunting of the host interferon response.

HCMV virion composition and genomes-to-pfu ratios. HCMV has a high particle-to-pfu ratio, producing several hundred to several thousand non-infectious particles for every infectious particle (102). A recombinant of strain AD169 deleted for US24 produced an equal number of genome containing particles, but showed a 20- to 30-fold reduction in infectivity and a ~10-fold higher genome-to-pfu ratio (134). Although no differences were seen in the limited amount of viral proteins assayed, the authors reasonably speculated that virion composition may have been altered in ΔUS24. Here we showed that ΔUS17 modulates the genome-to-pfu ratio in a different manner. This virus did not affect levels of infectious virus produced but produced larger numbers of genome-containing non-infectious particles (a net increase in total genome-containing particles). In comparisons of ΔUS17 virions with its parent or the US17v5 repair virus, levels of the virion glycoprotein gH were reduced and other differences in virion composition were noted by silver staining. The exact molecular composition required for infectivity of HCMV virions is not known; the ideal is likely to differ depending on the target cell or tissue and other physiological conditions. We are using mass spectroscopy to more precisely

define the molecular properties of ΔUS17 virions to further elucidate the relationship between virion composition and infectivity.

Glycoprotein H is part of the complex, gH/gL/gO, that is responsible for binding and entry into fibroblasts (135-137). Although we did observed reduced levels of gH incorporated into ΔUS17 virions, adsorption of individual virions was not altered as evidenced by the delivery of pp65 to host nuclei shortly after infection. Aside from their roles in virion entry, HCMV glycoproteins, especially gB and gH, elicit immune responses through induction of both nf-κB and Sp1 pathways shortly after binding to the host plasma membrane (128,138). This induction of the immune response has been linked to creation of a favorable environment inside the cell, facilitating the early stages of HCMV replication by up-regulating expression of key cellular transactivators. Therefore it is possible that the reduced levels of gH incorporated into ΔUS17 virions was not drastic enough to hinder virion entry but did contribute to an overall lack of fitness for any particular virion thus increasing the numbers of seemingly non-infectious virions during infection at high dilutions, i.e., limiting dilution plaque assay.

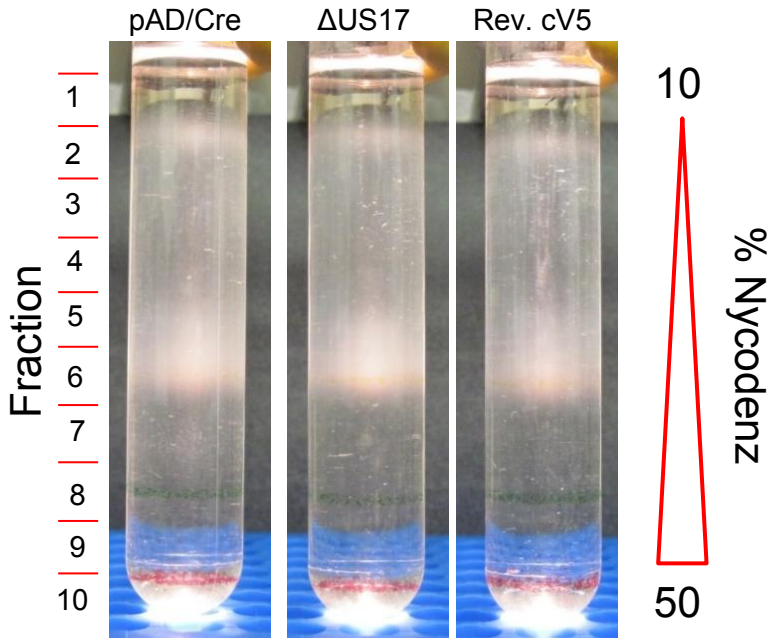

Figure 16**. Linear Nycodenz gradients of infected cell culture supernatants.** HFF were infected with either the parental virus (pAD/Cre), the US17 deletion virus ΔUS17, or the US17 deletion repair virus Rev. cV5 at an MOI of 0.01. 10 dpi, supernatants were clarified and thencentrifuged through a 10-50% Nycodenz gradient. Red lines indicate the approximate location of the 1 ml fraction boundaries. Yellow, red and green bands are density bead markers verifying that densities were equal between the three gradients.

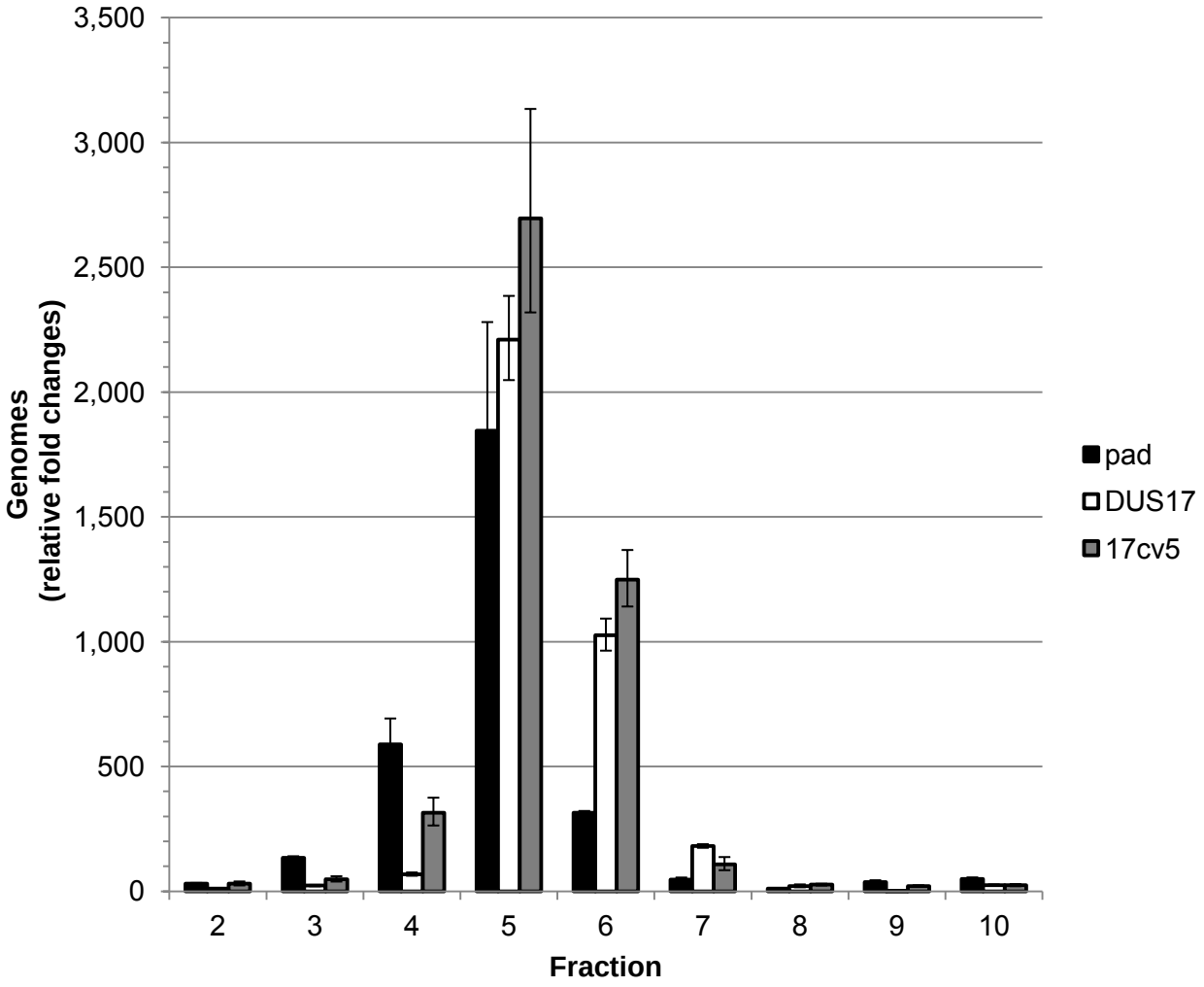

Figure 17. **HCMV genetic content of Nycodenz gradient fractions.** Samples of each fraction were Dnase I treated to remove non-encapsidated viral DNA. Viral genomes were extracted with a Qiagen Virus Mini-Elute kit and relative levels of genomes were measured via qPCR for HCMV UL83.

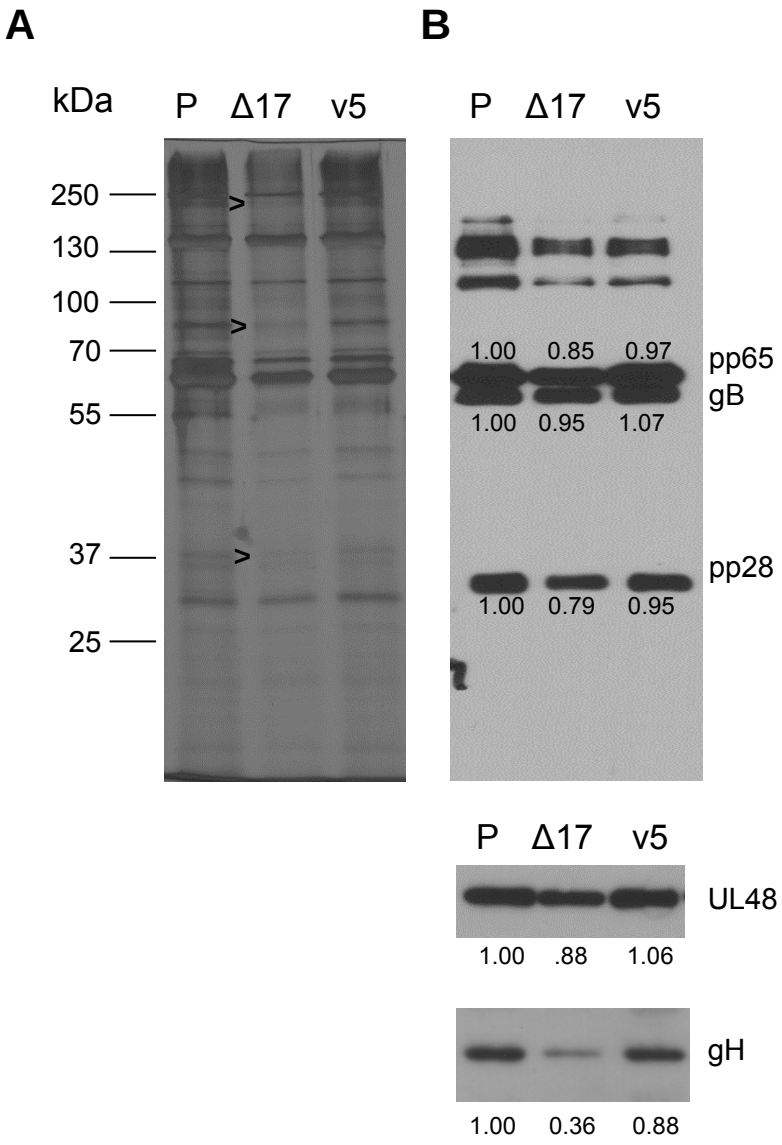

Figure 18. **ΔUS17 changes virion composition.** Supernatant associated virus from either the parental strain pAD/Cre (P), ΔUS17 (Δ17), or the repair virus (v5) was purified by centrifugation through a 10-50% Nycodenz gradient. Virion containing fractions were subsequently dialyzed into PBS analyzed for protein content. (A) Equal amounts of each sample were run on a 10% poly acrylamide gel and and silver stained. Subtle changes in the virion composition of ΔUS17 are noted as black arrows. (B) Immuno-blot for various structural proteins: pp65 (pUL83), gB (pUL55), pp28 (pUL99), Large tegument protein (pUL48) or gH (pUL75). Numbers underneath each blot are densitometric values calculated using image J software normalized to the parental sample.

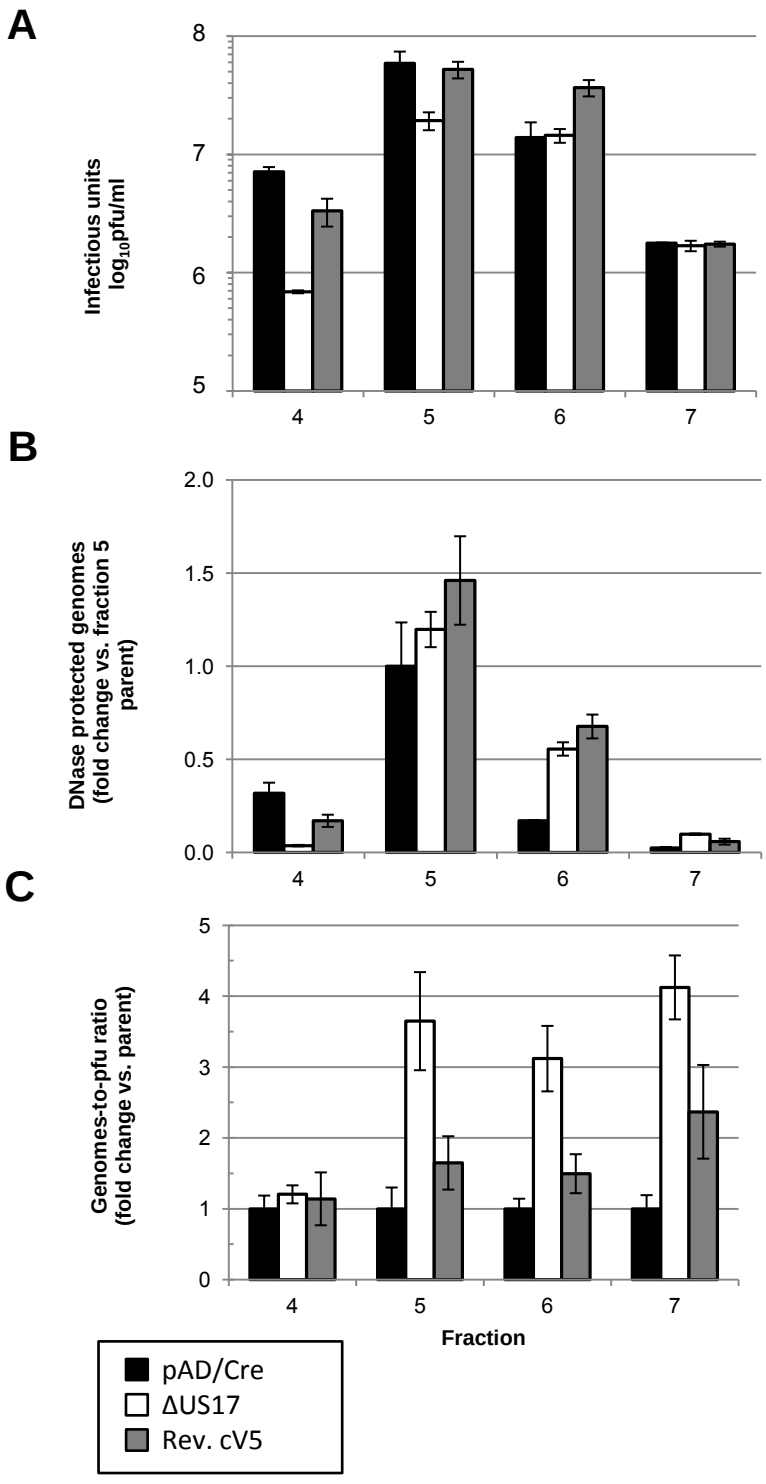

Figure 19. **ΔUS17 alters the genomes-to-pfu ratio of gradient purified virions** Gradient fractions (from Fig. 16) were plaque assayed for infectivity (A), or total DNAse I protected viral genomic content by qPCR (B). (C) Genomes-to-pfu ratios were calculated by dividing the ratios of the fold changes (vs. parent) of relative genomes and infectivity.

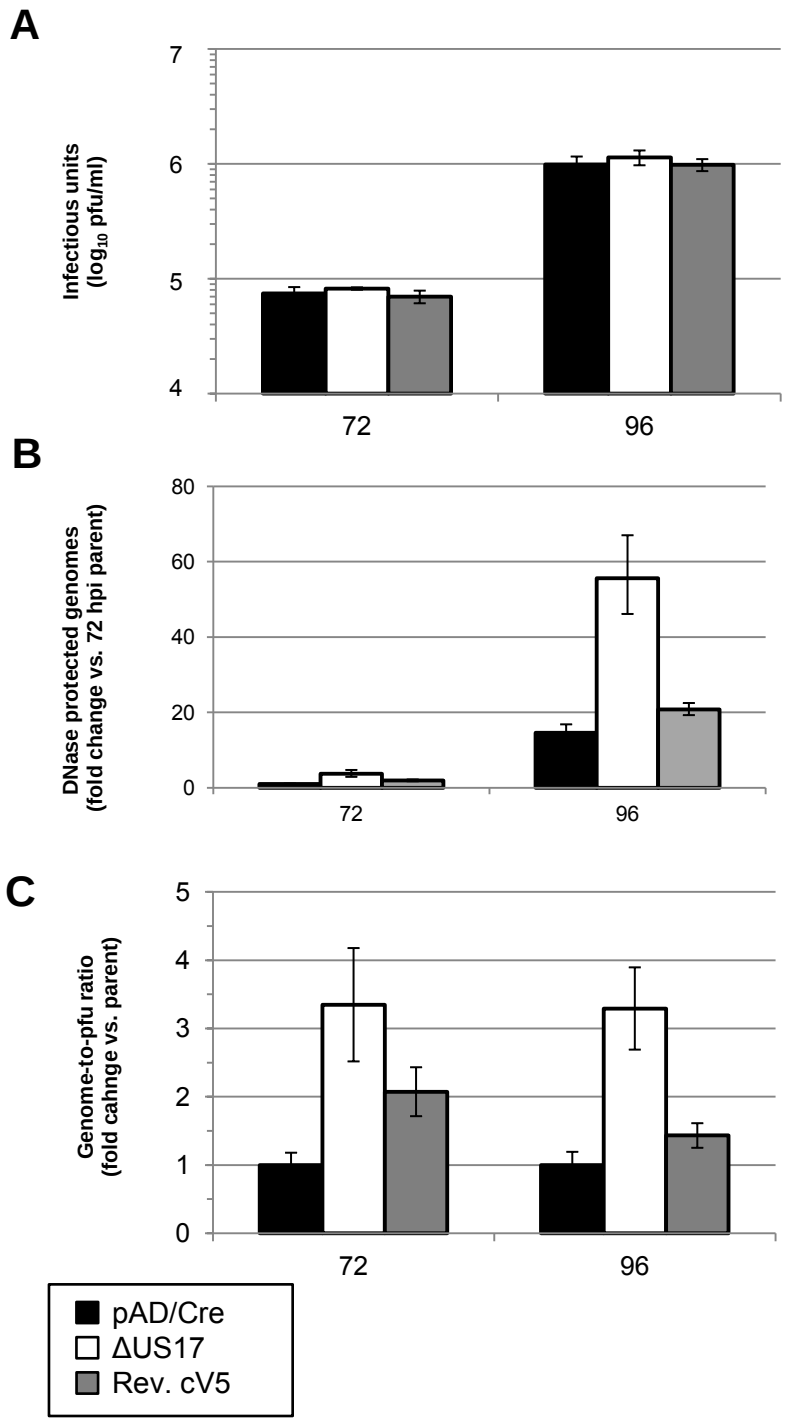

Figure 20. **ΔUS17 alters the genome-to-pfu ratio of infected cell culture supernatants.** Low passage HFF were infected at an MOI of 3.0 with either the parental virus, ΔUS17, or the US17-cV5 revertant virus. 72 and 96 hpi supernatants were harvested and plaque assayed for infectivity (A), or total DNAse protected viral genomic content by qPCR (B). C. Genome to pfu ratios were calculated by dividing the ratios of the fold changes (mutant vs. parent) of relative genomes and infectivity.

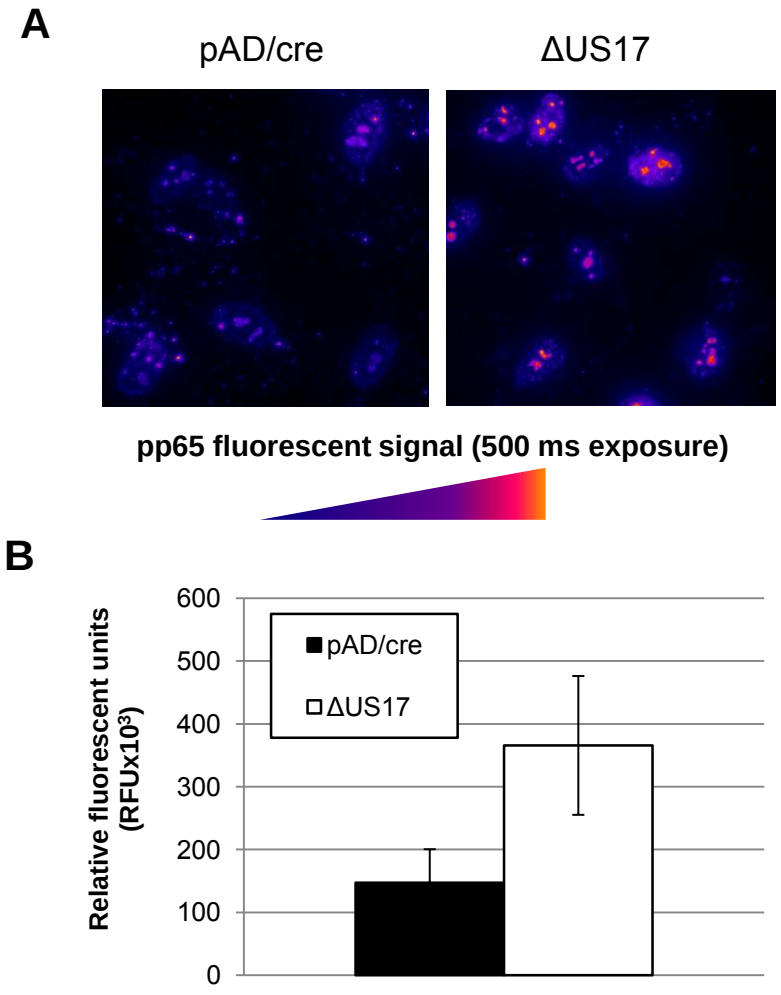

Figure 21. **Higher levels of tegument proteins are delivered per pfu to ΔUS17 infected fibroblasts.** HFF were infected in 8 well chamber slides with the indicated virus at MOI = 3.0. 2 hpi cells were washed with PBS, fixed in 4% paraformaldehyde and stained with a pp65 specific monoclonal antibody. (A) Representative images showing pp65 signals. (B) Average intensities and standard deviations of total pp65 fluorescent signal taken from three randomly chosen microscope fields from each of two independent biological experiments.

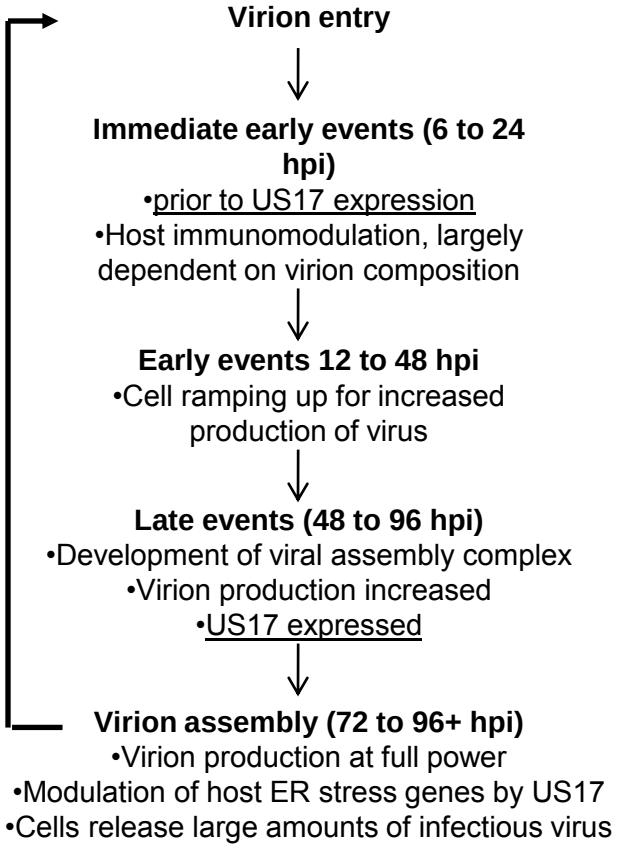

Figure 22. **Proposed model for US17 direct and indirect functions.** Timeline depicting US17's role as an indirect modulator of the host cell immune response at 12 hpi and a direct role for US17 at 96 hpi by way of modulation of host cell ER stress response genes.

Chapter Four

Conclusions and Discussion

This work highlights the complex and incompletely understood process that is HCMV immunomodulation and how factors such as virion composition can influence this process. In Chapter Two we demonstrated that ΔUS17 induced altered host transcriptional profiles from those of parental virions. At a very early time after infection (12 hpi) ΔUS17 elicited a reduced immune response from the host cell as evidenced by decreased production of transcripts associated with both interferon and innate immune responses. At a later time after infection (96 hpi) ΔUS17 differentially modulated transcripts encoding for genes involved in the ER stress response. In Chapter Three we further demonstrated that virions produced by ΔUS17 differed from parental virions, incorporating reduced amounts of the glycoprotein gH into their structure. ΔUS17 produced a >3-fold larger genome-to-pfu ratio while producing an equal number of infectious virus. When inoculated at an equal MOI this larger number of non-infectious particles produced by ΔUS17 delivered a ~3-fold larger amount of the tegument protein pp65 compared to parental. Additionally, UV inactivation of virions did not completely abrogate the transcriptional phenotype of ΔUS17 indicating that the structural differences of ΔUS17 virions contribute to the blunting of the host immune response (Data no shown).

At first, it seems counterintuitive that a virus would produce factors, such as US17, that increase the immunogenic properties of the virus thus making it more easily recognizable to the host's immune system. However, there is an accumulating body of work demonstrating that HCMV needs to strike a delicate balance of interferon and innate immune responses in order to ensure proper reproduction and survival (139-141).

HCMV has evolved the ability to interact with, and in some instances necessitates use of, host interferon response and anti-viral proteins. Two interferon inducible proteins, Viperin

(RSAD2) and IFI-16, enhance HCMV virion production and are specifically up-regulated by during infection. These same proteins inhibit replication of HIV, HCV, RSV and several other RNA viruses (142-146). HCMV utilizes IFI-16 in conjunction with pp65 as a trans-activator to up-regulate transcription of immediate early proteins thus aiding in the establishment of a lytic infection (113). RSAD2 interacts with another viral protein (UL37.1 vMIA) at the mitochondrial membrane to facilitate production of ATP (140,147,148). Upon knock-down of IFI-16 or Viperin, HCMV replicates less efficiently. In this way it appears that HCMV must counter-intuitively stimulate, and more importantly balance, the host immune response to ensure proper replication. If the immune response is activated too aggressively the cell will limit the spread of infection by initiating apoptosis of infected cells before production of progeny virions. In contrast, if there is too little immune response elicited by the virus, HCMV cannot initiate lytic replication efficiently.

This balance must be struck immediately upon infection before the host anti-viral response of the host cell overwhelms the virus and is therefore highly dependent on both virion structure and the particle–to-pfu ratio both of which are important mediators of host immune sensing. Therefore, it appears that HCMV has evolved US17 to modulate particle-to-pfu ratios and virion composition in order to produce virions that elicit the correct immune response from the host cell. Additionally the control of virion composition by US17 appears to be separate from viral pathways that are important for making the most basic unit of an infectious virion, i.e., ΔUS17 is replication competent in cell culture but the virions produced by ΔUS17 elicit an abnormal cellular response.

In addition to establishment of lytic replication, activation of the anti-viral response may be important for HCMV replication in another way. It has been reported that undifferentiated monocytes are an important reservoir of latently infected cells in the host (149-151). Monocytes

are a good viral reservoir because of their ability to travel throughout the body and deliver virus to distant sites from that of the primary infection. Upon differentiation of these monocytes into macrophage HCMV begins lytic replication and can then infect nearby cells of other lineages (fibroblasts, endo/epithelial cells etc)(152,153). Thus it is possible that HCMV uses US17 to control its immunomodulatory abilities through manipulation of particle-to-pfu ratios and virion composition in an effort to “bait” monocytes and other immune effecter cells to the site of a primary infection in order to establish latency. In fact, many of the most highly differentially expressed chemokines and cytokines that were seen to be down-modulated by ΔUS17 virions at 12 hpi, including cxcl10, ccl2, and ccl5, are known to be directly chemoattractive to monocytes (154-157) further strengthening this hypothesis .

In sum, the previously detailed experiments have elucidated a role for US17 in HCMV biology. We propose a model wherein US17 plays a role in the assembly of mature HCMV virions by modulating levels of genes involved in ER stress and the unfolded protein response at late times after infection thus affecting viral protein folding, trafficking, or incorporation into the virion structure in the cVAC(Fig. 23). Further, the involvement of US17 and possibly other US12 family members is important in the formation of particles that elicit an appropriate immune response from host cells.

REFERENCES

1. **Yu, X., S. Shah, M. Lee, W. Dai, P. Lo, W. Britt, H. Zhu, F. Liu, and Z. H. Zhou**. 2011. Biochemical and structural characterization of the capsid-bound tegument proteins of human cytomegalovirus. J.Struct.Biol. **174**:451-460

2. **Spear, P. G., M. T. Shieh, B. C. Herold, D. WuDunn, and T. I. Koshy**. 1992. Heparan sulfate glycosaminoglycans as primary cell surface receptors for herpes simplex virus. Adv.Exp.Med.Biol. **313**:341-353

3. **Sawitzky, D., A. Voigt, H. Zeichhardt, and K. O. Habermehl**. 1996. Glycoprotein B (gB) of pseudorabies virus interacts specifically with the glycosaminoglycan heparin. Virus Res. **41**:101-108

4. **Montgomery, R. I., M. S. Warner, B. J. Lum, and P. G. Spear**. 1996. Herpes simplex virus-1 entry into cells mediated by a novel member of the TNF/NGF receptor family. Cell **87**:427-436

5. **Feire, A. L., H. Koss, and T. Compton**. 2004. Cellular integrins function as entry receptors for human cytomegalovirus via a highly conserved disintegrin-like domain. Proc.Natl.Acad.Sci.U.S.A **101**:15470-15475

6. **Chan, G., M. T. Nogalski, and A. D. Yurochko**. 2009. Activation of EGFR on monocytes is required for human cytomegalovirus entry and mediates cellular motility. Proc.Natl.Acad.Sci.U.S.A **106**:22369-22374

7. **Ryckman, B. J., M. A. Jarvis, D. D. Drummond, J. A. Nelson, and D. C. Johnson**. 2006. Human cytomegalovirus entry into epithelial and endothelial cells depends on

genes UL128 to UL150 and occurs by endocytosis and low-pH fusion. J.Virol. **80**:710-722

8. **Compton, T., R. R. Nepomuceno, and D. M. Nowlin**. 1992. Human cytomegalovirus penetrates host cells by pH-independent fusion at the cell surface. Virology **191**:387-395

9. **Kalejta, R. F.** 2008. Tegument proteins of human cytomegalovirus. Microbiol.Mol.Biol.Rev. **72**:249-65, table

10. **Bauer, D. W., J. B. Huffman, F. L. Homa, and A. Evilevitch**. 2013. Herpes virus genome, the pressure is on. J.Am.Chem.Soc. **135**:11216-11221

11. **Harris, S. M., B. Bullock, E. Westgard, H. Zhu, R. M. Stenberg, and J. A. Kerry**. 2010. Functional properties of the human cytomegalovirus IE86 protein required for transcriptional regulation and virus replication. J.Virol. **84**:8839-8848

12. **Hagemeier, C., S. M. Walker, P. J. Sissons, and J. H. Sinclair**. 1992. The 72K IE1 and 80K IE2 proteins of human cytomegalovirus independently trans-activate the c-fos, c-myc and hsp70 promoters via basal promoter elements. J.Gen.Virol. **73 (Pt 9)**:2385-2393

13. **Yoo, Y. D., C. J. Chiou, K. S. Choi, Y. Yi, S. Michelson, S. Kim, G. S. Hayward, and S. J. Kim**. 1996. The IE2 regulatory protein of human cytomegalovirus induces expression of the human transforming growth factor beta1 gene through an Egr-1 binding site. J.Virol. **70**:7062-7070

14. **Paulus, C. and M. Nevels**. 2009. The human cytomegalovirus major immediate-early proteins as antagonists of intrinsic and innate antiviral host responses. Viruses. **1**:760-779

15. **Norris, K. L. and R. J. Youle**. 2008. Cytomegalovirus proteins vMIA and m38.5 link mitochondrial morphogenesis to Bcl-2 family proteins. J.Virol. **82**:6232-6243

16. **Sharon-Friling, R., J. Goodhouse, A. M. Colberg-Poley, and T. Shenk**. 2006. Human cytomegalovirus pUL37x1 induces the release of endoplasmic reticulum calcium stores. Proc.Natl.Acad.Sci.U.S.A **103**:19117-19122

17. **Hesse, J., S. Ameres, K. Besold, S. Krauter, A. Moosmann, and B. Plachter**. 2013. Suppression of CD8+ T-cell recognition in the immediate-early phase of human cytomegalovirus infection. J.Gen.Virol. **94**:376-386

18. **Sampaio, K. L., Y. Cavignac, Y. D. Stierhof, and C. Sinzger**. 2005. Human cytomegalovirus labeled with green fluorescent protein for live analysis of intracellular particle movements. J.Virol. **79**:2754-2767

19. **Sanchez, V. and D. H. Spector**. 2002. Virology. CMV makes a timely exit. Science **297**:778-779

20. **Klupp, B. G., H. Granzow, and T. C. Mettenleiter**. 2011. Nuclear envelope breakdown can substitute for primary envelopment-mediated nuclear egress of herpesviruses. J.Virol. **85**:8285-8292

21. **Mettenleiter, T. C.** 2004. Budding events in herpesvirus morphogenesis. Virus Res. **106**:167-180

22. **McMillan, T. N. and D. C. Johnson**. 2001. Cytoplasmic domain of herpes simplex virus gE causes accumulation in the trans-Golgi network, a site of virus envelopment and sorting of virions to cell junctions. J.Virol. **75**:1928-1940

23. **Remillard-Labrosse, G., C. Mihai, J. Duron, G. Guay, and R. Lippe**. 2009. Protein kinase D-dependent trafficking of the large Herpes simplex virus type 1 capsids from the TGN to plasma membrane. Traffic. **10**:1074-1083

24. **Tooze, J., M. Hollinshead, B. Reis, K. Radsak, and H. Kern**. 1993. Progeny vaccinia and human cytomegalovirus particles utilize early endosomal cisternae for their envelopes. Eur.J Cell Biol. **60**:163-178

25. **Cepeda, V., M. Esteban, and A. Fraile-Ramos**. 2010. Human cytomegalovirus final envelopment on membranes containing both trans-Golgi network and endosomal markers. Cell Microbiol. **12**:386-404

26. **Poole, E., A. Walther, K. Raven, C. A. Benedict, G. M. Mason, and J. Sinclair**. 2013. The myeloid transcription factor GATA-2 regulates the viral UL144 gene during human cytomegalovirus latency in an isolate-specific manner. J.Virol. **87**:4261-4271

27. **Reeves, M. B. and J. H. Sinclair**. 2010. Analysis of latent viral gene expression in natural and experimental latency models of human cytomegalovirus and its correlation with histone modifications at a latent promoter. J.Gen.Virol. **91**:599-604

28. **Farrell, M. J., A. T. Dobson, and L. T. Feldman**. 1991. Herpes simplex virus latency-associated transcript is a stable intron. Proc.Natl.Acad.Sci.U.S.A **88**:790-794

29. **Wigdahl, B. L., R. J. Ziegler, M. Sneve, and F. Rapp**. 1983. Herpes simplex virus latency and reactivation in isolated rat sensory neurons. Virology **127**:159-167

30. **Levine, M., A. L. Goldin, and J. C. Glorioso**. 1980. Persistence of herpes simplex virus genes in cells of neuronal origin. J.Virol. **35**:203-210

31. **Hargett, D. and T. E. Shenk**. 2010. Experimental human cytomegalovirus latency in CD14+ monocytes. Proc.Natl.Acad.Sci.U.S.A **107**:20039-20044

32. **Sindre, H., G. E. Tjoonnfjord, H. Rollag, T. Ranneberg-Nilsen, O. P. Veiby, S. Beck, M. Degre, and K. Hestdal**. 1996. Human cytomegalovirus suppression of and latency in early hematopoietic progenitor cells. Blood **88**:4526-4533

33. **Babcock, G. J., L. L. Decker, M. Volk, and D. A. Thorley-Lawson**. 1998. EBV persistence in memory B cells in vivo. Immunity. **9**:395-404

34. **Boppana, S. B. and K. B. Fowler**. 2007. Persistence in the population: epidemiology and transmisson, *In*.

35. **Staras, S. A., S. C. Dollard, K. W. Radford, W. D. Flanders, R. F. Pass, and M. J. Cannon**. 2006. Seroprevalence of cytomegalovirus infection in the United States, 1988-1994. Clin.Infect.Dis. **43**:1143-1151

36. **Janssen, H. P., A. M. van Loon, M. J. Meddens, E. C. Eickmans-Josten, A. J. Hoitsma, T. J. de Witte, and W. G. Quint**. 1988. Immunological detection of cytomegalovirus early antigen on monolayers inoculated with urine specimens by centrifugation and cultured for 6 days as alternative to conventional virus isolation. J.Clin.Microbiol. **26**:1313-1315

37. **Chou, S. and T. C. Merigan**. 1983. Rapid detection and quantitation of human cytomegalovirus in urine through DNA hybridization. N.Engl.J.Med. **308**:921-925

38. **Tamura, T., S. Chiba, Y. Chiba, and T. Nakao**. 1980. Virus excretion and neutralizing antibody response in saliva in human cytomegalovirus infection. Infect.Immun. **29**:842-845

39. **Sugar, E. A., D. A. Jabs, A. Ahuja, J. E. Thorne, R. P. Danis, and C. L. Meinert**. 2012. Incidence of cytomegalovirus retinitis in the era of highly active antiretroviral therapy. Am.J.Ophthalmol. **153**:1016-1024

40. **Tyms, A. S., D. L. Taylor, and J. M. Parkin**. 1989. Cytomegalovirus and the acquired immunodeficiency syndrome. J.Antimicrob.Chemother. **23 Suppl A**:89-105

41. **Larsson, K., J. Aschan, M. Remberger, O. Ringden, J. Winiarski, and P. Ljungman**. 2004. Reduced risk for extensive chronic graft-versus-host disease in patients receiving transplants with human leukocyte antigen-identical sibling donors given polymerase chain reaction-based preemptive therapy against cytomegalovirus. Transplantation **77**:526-531

42. **Onor, I. O., S. B. Todd, E. Meredith, S. D. Perez, A. K. Mehta, L. G. Marshall, S. J. Knechtle, and S. I. Hanish**. 2013. Evaluation of clinical outcomes of prophylactic versus preemptive cytomegalovirus strategy in liver transplant recipients. Transpl.Int. **26**:592-600

43. **Roux, A., G. Mourin, S. Fastenackels, J. R. Almeida, M. C. Iglesias, A. Boyd, E. Gostick, M. Larsen, D. A. Price, K. Sacre, D. C. Douek, B. Autran, C. Picard, S. Miranda, D. Sauce, M. Stern, and V. Appay**. 2013. CMV driven CD8(+) T-cell activation is associated with acute rejection in lung transplantation. Clin.Immunol. **148**:16-26

44. **Allard, M., P. Tonnerre, S. Nedellec, R. Oger, A. Morice, Y. Guilloux, E. Houssaint, B. Charreau, and N. Gervois**. 2012. HLA-E-restricted cross-recognition of allogeneic endothelial cells by CMV-associated CD8 T cells: a potential risk factor following transplantation. PLoS.One. **7**:e50951

45. **Iwaszko, M. and K. Bogunia-Kubik**. 2011. Clinical significance of the HLA-E and CD94/NKG2 interaction. Arch.Immunol.Ther.Exp.(Warsz.) **59**:353-367

46. **Cannon, M. J.** 2009. Congenital cytomegalovirus (CMV) epidemiology and awareness. J.Clin.Virol. **46 Suppl 4**:S6-10

47. **Demmler, G. J.** 1996. Congenital cytomegalovirus infection and disease. Adv.Pediatr.Infect.Dis. **11**:135-162

48. **Stagno, S., R. F. Pass, G. Cloud, W. J. Britt, R. E. Henderson, P. D. Walton, D. A. Veren, F. Page, and C. A. Alford**. 1986. Primary cytomegalovirus infection in pregnancy. Incidence, transmission to fetus, and clinical outcome. Journal of the American Medical Association **256**:1904-1908

49. **Mocarski, E. S., T. Shenk, R. F. Pass, and D. G. Paul**. 2013. Cytomegaloviruses, p. 1960-2014. *In*: D. M. Knipe, P. M. Howley, D. E. Griffin, R. A. Lamb, M. A. Martin, B. Roizman, I. C. Jeffrey, and R. R. Vincent (eds.), Fields Virology. 6 ed. Lippincott Williams & Wilkins, Philadelphia.

50. **Manicklal, S., V. C. Emery, T. Lazzarotto, S. B. Boppana, and R. K. Gupta**. 2013. The "silent" global burden of congenital cytomegalovirus. Clin.Microbiol.Rev. **26**:86-102

51. **Murphy, E., D. Yu, J. Grimwood, J. Schmutz, M. Dickson, M. A. Jarvis, G. Hahn, J. A. Nelson, R. M. Myers, and T. E. Shenk**. 2003. Coding potential of laboratory and clinical strains of human cytomegalovirus. Proc.Natl.Acad.Sci.U.S.A **100**:14976-14981

52. **Davison, A. J., A. Dolan, P. Akter, C. Addison, D. J. Dargan, D. J. Alcendor, D. J. McGeoch, and G. S. Hayward**. 2003. The human cytomegalovirus genome revisited: comparison with the chimpanzee cytomegalovirus genome. J.Gen.Virol. **84**:17-28

53. **Stern-Ginossar, N., B. Weisburd, A. Michalski, V. T. Le, M. Y. Hein, S. X. Huang, M. Ma, B. Shen, S. B. Qian, H. Hengel, M. Mann, N. T. Ingolia, and J. S. Weissman**. 2012. Decoding human cytomegalovirus. Science **338**:1088-1093

54. **Dhuruvasan, K., G. Sivasubramanian, and P. E. Pellett**. 2010. Roles of host and viral microRNAs in human cytomegalovirus biology. Virus Res.

55. **Grey, F. and J. Nelson**. 2008. Identification and function of human cytomegalovirus microRNAs. J.Clin.Virol. **41**:186-191

56. **Grey, F., H. Meyers, E. A. White, D. H. Spector, and J. Nelson**. 2007. A human cytomegalovirus-encoded microRNA regulates expression of multiple viral genes involved in replication. PLoS.Pathog. **3**:e163

57. **Dolan, A., C. Cunningham, R. D. Hector, A. F. Hassan-Walker, L. Lee, C. Addison, D. J. Dargan, D. J. McGeoch, D. Gatherer, V. C. Emery, P. D. Griffiths, C. Sinzger, B. P. McSharry, G. W. Wilkinson, and A. J. Davison**. 2004. Genetic content of wild-type human cytomegalovirus. J.Gen.Virol. **85**:1301-1312

58. **Yu, D., M. C. Silva, and T. Shenk**. 2003. Functional map of human cytomegalovirus AD169 defined by global mutational analysis. Proc.Natl.Acad.Sci.U.S.A **100**:12396-12401

59. **Mocarski, E. S., Jr.** 2002. Immunomodulation by cytomegaloviruses: manipulative strategies beyond evasion. Trends Microbiol. **10**:332-339

60. **Umashankar, M., A. Petrucelli, L. Cicchini, P. Caposio, C. N. Kreklywich, M. Rak, F. Bughio, D. C. Goldman, K. L. Hamlin, J. A. Nelson, W. H. Fleming, D. N. Streblow,**

and F. Goodrum. 2011. A novel human cytomegalovirus locus modulates cell type-specific outcomes of infection. PLoS.Pathog. **7**:e1002444

61. **Bughio, F., D. A. Elliott, and F. Goodrum**. 2013. An endothelial cell-specific requirement for the UL133-UL138 locus of human cytomegalovirus for efficient virus maturation. J.Virol. **87**:3062-3075

62. **Lin, Y. L., P. C. Chang, Y. Wang, and M. Li**. 2008. Identification of novel viral interleukin-10 isoforms of human cytomegalovirus AD169. Virus Res. **131**:213-223

63. **Lockridge, K. M., S. S. Zhou, R. H. Kravitz, J. L. Johnson, E. T. Sawai, E. L. Blewett, and P. A. Barry**. 2000. Primate cytomegaloviruses encode and express an IL-10-like protein. Virology **268**:272-280

64. **Tomasec, P., E. C. Wang, A. J. Davison, B. Vojtesek, M. Armstrong, C. Griffin, B. P. McSharry, R. J. Morris, S. Llewellyn-Lacey, C. Rickards, A. Nomoto, C. Sinzger, and G. W. Wilkinson**. 2005. Downregulation of natural killer cell-activating ligand CD155 by human cytomegalovirus UL141. Nat.Immunol. **6**:181-188

65. **Luttichau, H. R.** 2010. The cytomegalovirus UL146 gene product vCXCL1 targets both CXCR1 and CXCR2 as an agonist. J.Biol.Chem. **285**:9137-9146

66. **Weston, K. and B. G. Barrell**. 1986. Sequence of the short unique region, short repeats, and part of the long repeats of human cytomegalovirus. J Mol.Biol. **192**:177-208

67. **Chee, M. S., A. T. Bankier, S. Beck, R. Bohni, C. M. Brown, R. Cerny, T. Horsnell, C. A. Hutchison, T. Kouzarides, J. A. Martignetti, E. Preddie, S. C. Satchwell, P. Tomlinson, K. M. Weston, and B. G. Barrell**. 1990. Analysis of the protein-coding

content of the sequence of human cytomegalovirus strain AD169. Curr.Top.Microbiol.Immunol. **154**:125-169

68. **Carrara, G., N. Saraiva, C. Gubser, B. F. Johnson, and G. L. Smith**. 2012. Six-transmembrane topology for Golgi anti-apoptotic protein (GAAP) and Bax inhibitor 1 (BI-1) provides model for the transmembrane Bax inhibitor-containing motif (TMBIM) family. J.Biol.Chem. **287**:15896-15905

69. **Das, S. and P. E. Pellett**. 2007. Members of the HCMV US12 family of predicted heptaspanning membrane proteins have unique intracellular distributions, including association with the cytoplasmic virion assembly complex. Virology **361**:263-273

70. **Das, S., Y. Skomorovska-Prokvolit, F. Z. Wang, and P. E. Pellett**. 2006. Infection-dependent nuclear localization of US17, a member of the US12 family of human cytomegalovirus-encoded seven-transmembrane proteins. J.Virol. **80**:1191-1203

71. **Lesniewski, M., S. Das, Y. Skomorovska-Prokvolit, F. Z. Wang, and P. E. Pellett**. 2006. Primate cytomegalovirus US12 gene family: A distinct and diverse clade of seven-transmembrane proteins. Virology **354**:286-298

72. **Chee, M. S., S. C. Satchwell, E. Preddie, K. M. Weston, and B. G. Barrell**. 1990. Human cytomegalovirus encodes three G protein-coupled receptor homologues. Nature **344**:774-777

73. **Dunn, W., C. Chou, H. Li, R. Hai, D. Patterson, V. Stolc, H. Zhu, and F. Liu**. 2003. Functional profiling of a human cytomegalovirus genome. Proc.Natl.Acad.Sci.U.S.A **100**:14223-14228

74. **Hai, R., A. Chu, H. Li, S. Umamoto, P. Rider, and F. Liu**. 2006. Infection of human cytomegalovirus in cultured human gingival tissue. Virol.J. **3**:84

75. **Bronzini, M., A. Luganini, V. Dell'oste, A. M. De, S. Landolfo, and G. Gribaudo**. 2012. The US16 gene of Human Cytomegalovirus is Required for Efficient Viral Infection of Endothelial and Epithelial Cells. J.Virol.

76. **Wang, D., Q. C. Yu, J. Schroer, E. Murphy, and T. Shenk**. 2007. Human cytomegalovirus uses two distinct pathways to enter retinal pigmented epithelial cells. Proc.Natl.Acad.Sci.U.S.A **104**:20037-20042

77. **Vanarsdall, A. L., M. C. Chase, and D. C. Johnson**. 2011. Human cytomegalovirus glycoprotein gO complexes with gH/gL, promoting interference with viral entry into human fibroblasts but not entry into epithelial cells. J.Virol. **85**:11638-11645

78. **Schmolke, S., H. F. Kern, P. Drescher, G. Jahn, and B. Plachter**. 1995. The dominant phosphoprotein pp65 (UL83) of human cytomegalovirus is dispensable for growth in cell culture. J.Virol. **69**:5959-5968

79. **Chevillotte, M., S. Landwehr, L. Linta, G. Frascaroli, A. Luske, C. Buser, T. Mertens, and E. J. von**. 2009. Major tegument protein pp65 of human cytomegalovirus is required for the incorporation of pUL69 and pUL97 into the virus particle and for viral growth in macrophages. J.Virol. **83**:2480-2490

80. **Watanabe, N. and E. Lam**. 2008. Arabidopsis Bax inhibitor-1: A rheostat for ER stress-induced programmed cell death. Plant Signal.Behav. **3**:564-566

81. **Rojas-Rivera, D., R. Armisen, A. Colombo, G. Martinez, A. L. Eguiguren, A. Diaz, S. Kiviluoto, D. Rodriguez, M. Patron, R. Rizzuto, G. Bultynck, M. L. Concha, J.**

Sierralta, A. Stutzin, and C. Hetz. 2012. TMBIM3/GRINA is a novel unfolded protein response (UPR) target gene that controls apoptosis through the modulation of ER calcium homeostasis. Cell Death.Differ.

82. **de, M. F., C. Gubser, M. M. van Dommelen, H. J. Visch, F. Distelmaier, A. Postigo, T. Luyten, J. B. Parys, S. H. de, G. L. Smith, P. H. Willems, and F. J. van Kuppeveld**. 2009. Human Golgi antiapoptotic protein modulates intracellular calcium fluxes. Mol.Biol Cell **20**:3638-3645

83. **Kim, H. R., G. H. Lee, K. C. Ha, T. Ahn, J. Y. Moon, B. J. Lee, S. G. Cho, S. Kim, Y. R. Seo, Y. J. Shin, S. W. Chae, J. C. Reed, and H. J. Chae**. 2008. Bax Inhibitor-1 Is a pH-dependent regulator of Ca2+ channel activity in the endoplasmic reticulum. J Biol Chem. **283**:15946-15955

84. **Xu, C., W. Xu, A. E. Palmer, and J. C. Reed**. 2008. BI-1 regulates endoplasmic reticulum Ca2+ homeostasis downstream of Bcl-2 family proteins. J Biol Chem. **283**:11477-11484

85. **Bultynck, G., S. Kiviluoto, N. Henke, H. Ivanova, L. Schneider, V. Rybalchenko, T. Luyten, K. Nuyts, B. W. De, I. Bezprozvanny, J. B. Parys, S. H. de, L. Missiaen, and A. Methner**. 2012. The C terminus of Bax inhibitor-1 forms a Ca2+-permeable channel pore. J.Biol.Chem. **287**:2544-2557

86. **Lisbona, F., D. Rojas-Rivera, P. Thielen, S. Zamorano, D. Todd, F. Martinon, A. Glavic, C. Kress, J. H. Lin, P. Walter, J. C. Reed, L. H. Glimcher, and C. Hetz**. 2009. BAX inhibitor-1 is a negative regulator of the ER stress sensor IRE1alpha. Mol.Cell **33**:679-691

87. **Bailly-Maitre, B., B. F. Belgardt, S. D. Jordan, B. Coornaert, M. J. von Freyend, A. Kleinridders, J. Mauer, M. Cuddy, C. L. Kress, D. Willmes, M. Essig, B. Hampel, U. Protzer, J. C. Reed, and J. C. Bruning**. 2010. Hepatic Bax inhibitor-1 inhibits IRE1alpha and protects from obesity-associated insulin resistance and glucose intolerance. J.Biol.Chem. **285**:6198-6207

88. **Xu, C., W. Xu, A. E. Palmer, and J. C. Reed**. 2008. BI-1 regulates endoplasmic reticulum Ca2+ homeostasis downstream of Bcl-2 family proteins. J.Biol.Chem. **283**:11477-11484

89. **Kiviluoto, S., L. Schneider, T. Luyten, T. Vervliet, L. Missiaen, S. H. de, J. B. Parys, A. Methner, and G. Bultynck**. 2012. Bax inhibitor-1 is a novel IP(3) receptor-interacting and -sensitizing protein. Cell Death.Dis. **3**:e367

90. **Sano, R., Y. C. Hou, M. Hedvat, R. G. Correa, C. W. Shu, M. Krajewska, P. W. Diaz, C. M. Tamble, G. Quarato, R. A. Gottlieb, M. Yamaguchi, V. Nizet, R. Dahl, D. D. Thomas, S. W. Tait, D. R. Green, P. B. Fisher, S. Matsuzawa, and J. C. Reed**. 2012. Endoplasmic reticulum protein BI-1 regulates Ca(2)(+)-mediated bioenergetics to promote autophagy. Genes Dev. **26**:1041-1054

91. **Saraiva, N., D. L. Prole, G. Carrara, B. F. Johnson, C. W. Taylor, M. Parsons, and G. L. Smith**. 2013. hGAAP promotes cell adhesion and migration via the stimulation of store-operated Ca2+ entry and calpain 2. J.Cell Biol. **202**:699-713

92. **Gubser, C., D. Bergamaschi, M. Hollinshead, X. Lu, F. J. van Kuppeveld, and G. L. Smith**. 2007. A new inhibitor of apoptosis from vaccinia virus and eukaryotes. PLoS.Pathog. **3**:e17

93. **Saraiva, N., D. L. Prole, G. Carrara, M. C. Maluquer de, B. F. Johnson, B. Byrne, C. W. Taylor, and G. L. Smith**. 2013. Human and viral Golgi anti-apoptotic proteins (GAAPs) oligomerize via different mechanisms and monomeric GAAP inhibits apoptosis and modulates calcium. J.Biol.Chem. **288**:13057-13067

94. **Gibson, W.** 2008. Structure and formation of the cytomegalovirus virion. Curr.Top.Microbiol.Immunol. **325**:187-204

95. **Varnum, S. M., D. N. Streblow, M. E. Monroe, P. Smith, K. J. Auberry, L. Pasa-Tolic, D. Wang, D. G. Camp, K. Rodland, S. Wiley, W. Britt, T. Shenk, R. D. Smith, and J. A. Nelson**. 2004. Identification of proteins in human cytomegalovirus (HCMV) particles: the HCMV proteome. J.Virol. **78**:10960-10966

96. **Das, S., A. Vasanji, and P. E. Pellett**. 2007. Three-dimensional structure of the human cytomegalovirus cytoplasmic virion assembly complex includes a reoriented secretory apparatus. J.Virol. **81**:11861-11869

97. **Sanchez, V., K. D. Greis, E. Sztul, and W. J. Britt**. 2000. Accumulation of virion tegument and envelope proteins in a stable cytoplasmic compartment during human cytomegalovirus replication: characterization of a potential site of virus assembly. J.Virol. **74**:975-986

98. **Sanchez, V., E. Sztul, and W. J. Britt**. 2000. Human cytomegalovirus pp28 (UL99) localizes to a cytoplasmic compartment which overlaps the endoplasmic reticulum-golgi-intermediate compartment. J.Virol. **74**:3842-3851

99. **Theiler, R. N. and T. Compton**. 2002. Distinct glycoprotein O complexes arise in a post-Golgi compartment of cytomegalovirus-infected cells. J.Virol. **76**:2890-2898

100. **AuCoin, D. P., G. B. Smith, C. D. Meiering, and E. S. Mocarski**. 2006. Betaherpesvirus-conserved cytomegalovirus tegument protein ppUL32 (pp150) controls cytoplasmic events during virion maturation. J.Virol. **80**:8199-8210

101. **Tandon, R. and E. S. Mocarski**. 2008. Control of cytoplasmic maturation events by cytomegalovirus tegument protein pp150. J.Virol. **82**:9433-9444

102. **Benyesh-Melnick, M., F. Probstmeyer, R. McCombs, J. P. Brunschwig, and V. Vonka**. 1966. Correlation between infectivity and physical virus particles in human cytomegalovirus. J.Bacteriol. **92**:1555-1561

103. **Pepperl, S., J. Munster, M. Mach, J. R. Harris, and B. Plachter**. 2000. Dense bodies of human cytomegalovirus induce both humoral and cellular immune responses in the absence of viral gene expression. J.Virol. **74**:6132-6146

104. **Irmiere, A. and W. Gibson**. 1983. Isolation and characterization of a noninfectious virion-like particle released from cells infected with human strains of cytomegalovirus. Virology **130**:118-133

105. **Ahlqvist, J. and E. Mocarski**. 2011. Cytomegalovirus UL103 controls virion and dense body egress. J.Virol.

106. **Isler, J. A., A. H. Skalet, and J. C. Alwine**. 2005. Human cytomegalovirus infection activates and regulates the unfolded protein response. J.Virol. **79**:6890-6899

107. **Isler, J. A., T. G. Maguire, and J. C. Alwine**. 2005. Production of infectious human cytomegalovirus virions is inhibited by drugs that disrupt calcium homeostasis in the endoplasmic reticulum. J.Virol. **79**:15388-15397

108. **Xuan, B., Z. Qian, E. Torigoi, and D. Yu**. 2009. Human cytomegalovirus protein pUL38 induces ATF4 expression, inhibits persistent JNK phosphorylation, and suppresses endoplasmic reticulum stress-induced cell death. J.Virol. **83**:3463-3474

109. **Meunier, L., Y. K. Usherwood, K. T. Chung, and L. M. Hendershot**. 2002. A subset of chaperones and folding enzymes form multiprotein complexes in endoplasmic reticulum to bind nascent proteins. Mol.Biol.Cell **13**:4456-4469

110. **Buchkovich, N. J., T. G. Maguire, Y. Yu, A. W. Paton, J. C. Paton, and J. C. Alwine**. 2008. Human cytomegalovirus specifically controls the levels of the endoplasmic reticulum chaperone BiP/GRP78, which is required for virion assembly. J.Virol. **82**:31-39

111. **Munger, J., B. D. Bennett, A. Parikh, X. J. Feng, J. McArdle, H. A. Rabitz, T. Shenk, and J. D. Rabinowitz**. 2008. Systems-level metabolic flux profiling identifies fatty acid synthesis as a target for antiviral therapy. Nat.Biotechnol. **26**:1179-1186

112. **Buchkovich, N. J., T. G. Maguire, and J. C. Alwine**. 2010. Role of the endoplasmic reticulum chaperone BiP, SUN domain proteins, and dynein in altering nuclear morphology during human cytomegalovirus infection. J.Virol. **84**:7005-7017

113. **Cristea, I. M., N. J. Moorman, S. S. Terhune, C. D. Cuevas, E. S. O'Keefe, M. P. Rout, B. T. Chait, and T. Shenk**. 2010. Human cytomegalovirus pUL83 stimulates activity of the viral immediate-early promoter through its interaction with the cellular IFI16 protein. J.Virol. **84**:7803-7814

114. **Abate, D. A., S. Watanabe, and E. S. Mocarski**. 2004. Major human cytomegalovirus structural protein pp65 (ppUL83) prevents interferon response factor 3 activation in the interferon response. J.Virol. **78**:10995-11006

115. **Lee, E. C., D. Yu, d. Martinez, V, L. Tessarollo, D. A. Swing, Court DL, N. A. Jenkins, and N. G. Copeland**. 2001. A highly efficient Escherichia coli-based chromosome engineering system adapted for recombinogenic targeting and subcloning of BAC DNA. Genomics **73**:56-65

116. **Warming, S., N. Costantino, Court DL, N. A. Jenkins, and N. G. Copeland**. 2005. Simple and highly efficient BAC recombineering using galK selection. Nucleic Acids Res. **33**:e36

117. **Qian, Z., B. Xuan, T. T. Hong, and D. Yu**. 2008. The full-length protein encoded by human cytomegalovirus gene UL117 is required for the proper maturation of viral replication compartments. J.Virol. **82**:3452-3465

118. **Tusher, V. G., R. Tibshirani, and G. Chu**. 2001. Significance analysis of microarrays applied to the ionizing radiation response. Proc.Natl.Acad.Sci.U.S.A **98**:5116-5121

119. **Maere, S., K. Heymans, and M. Kuiper**. 2005. BiNGO: a Cytoscape plugin to assess overrepresentation of gene ontology categories in biological networks. Bioinformatics. **21**:3448-3449

120. **Guo, Y. W. and E. S. Huang**. 1993. Characterization of a structurally tricistronic gene of human cytomegalovirus composed of U(s)18, U(s)19, and U(s)20. J.Virol. **67**:2043-2054

121. **Miller, M. S., W. E. Furlong, L. Pennell, M. Geadah, and L. Hertel**. 2010. RASCAL is a new human cytomegalovirus-encoded protein that localizes to the nuclear lamina and in cytoplasmic vesicles at late times postinfection. J.Virol. **84**:6483-6496

122. **Dittmer, D. and E. S. Mocarski**. 1997. Human cytomegalovirus infection inhibits G1/S transition. J.Virol. **71**:1629-1634

123. **Fortunato, E. A., V. Sanchez, J. Y. Yen, and D. H. Spector**. 2002. Infection of cells with human cytomegalovirus during S phase results in a blockade to immediate-early gene expression that can be overcome by inhibition of the proteasome. J.Virol. **76**:5369-5379

124. **Du, P., W. A. Kibbe, and S. M. Lin**. 2008. lumi: a pipeline for processing Illumina microarray. Bioinformatics. **24**:1547-1548

125. **Buchkovich, N. J., T. G. Maguire, A. W. Paton, J. C. Paton, and J. C. Alwine**. 2009. The endoplasmic reticulum chaperone BiP/GRP78 is important in the structure and function of the HCMV assembly compartment. J.Virol.

126. **Simmen, K. A., J. Singh, B. G. Luukkonen, M. Lopper, A. Bittner, N. E. Miller, M. R. Jackson, T. Compton, and K. Fruh**. 2001. Global modulation of cellular transcription by human cytomegalovirus is initiated by viral glycoprotein B. Proc.Natl.Acad.Sci.U.S.A **98**:7140-7145

127. **Boehme, K. W., M. Guerrero, and T. Compton**. 2006. Human cytomegalovirus envelope glycoproteins B and H are necessary for TLR2 activation in permissive cells. J.Immunol. **177**:7094-7102

128. **Yurochko, A. D., E. S. Hwang, L. Rasmussen, S. Keay, L. Pereira, and E. S. Huang**. 1997. The human cytomegalovirus UL55 (gB) and UL75 (gH) glycoprotein ligands initiate the rapid activation of Sp1 and NF-kappaB during infection. J.Virol. **71**:5051-5059

129. **Guo, F. J., Y. Liu, J. Zhou, S. Luo, W. Zhao, X. Li, and C. Liu**. 2012. XBP1S protects cells from ER stress-induced apoptosis through Erk1/2 signaling pathway involving CHOP. Histochem.Cell Biol. **138**:447-460

130. **Mungrue, I. N., J. Pagnon, O. Kohannim, P. S. Gargalovic, and A. J. Lusis**. 2009. CHAC1/MGC4504 is a novel proapoptotic component of the unfolded protein response, downstream of the ATF4-ATF3-CHOP cascade. J.Immunol. **182**:466-476

131. **Teske, B. F., M. E. Fusakio, D. Zhou, J. Shan, J. N. McClintick, M. S. Kilberg, and R. C. Wek**. 2013. CHOP induces activating transcription factor 5 (ATF5) to trigger apoptosis in response to perturbations in protein homeostasis. Mol.Biol.Cell **24**:2477-2490

132. **Lee, G. H., H. K. Kim, S. W. Chae, D. S. Kim, K. C. Ha, M. Cuddy, C. Kress, J. C. Reed, H. R. Kim, and H. J. Chae**. 2007. Bax inhibitor-1 regulates endoplasmic reticulum stress-associated reactive oxygen species and heme oxygenase-1 expression. J.Biol.Chem. **282**:21618-21628

133. **Hayajneh, W. A., A. M. Colberg-Poley, A. Skaletskaya, L. M. Bartle, M. M. Lesperance, D. G. Contopoulos-Ioannidis, N. L. Kedersha, and V. S. Goldmacher**. 2001. The sequence and antiapoptotic functional domains of the human cytomegalovirus UL37 exon 1 immediate early protein are conserved in multiple primary strains. Virology **279**:233-240

134. **Feng, X., J. Schroer, D. Yu, and T. Shenk**. 2006. Human cytomegalovirus pUS24 is a virion protein that functions very early in the replication cycle. J.Virol. **80**:8371-8378

135. **Wang, D. and T. Shenk**. 2005. Human cytomegalovirus virion protein complex required for epithelial and endothelial cell tropism. Proc.Natl.Acad.Sci.U.S.A **102**:18153-18158

136. **Baldwin, B. R., C. O. Zhang, and S. Keay**. 2000. Cloning and epitope mapping of a functional partial fusion receptor for human cytomegalovirus gH. J.Gen.Virol. **81**:27-35

137. **Ryckman, B. J., M. C. Chase, and D. C. Johnson**. 2008. HCMV gH/gL/UL128-131 interferes with virus entry into epithelial cells: evidence for cell type-specific receptors. Proc.Natl.Acad.Sci.U.S.A **105**:14118-14123

138. **Yurochko, A. D. and E. S. Huang**. 1999. Human cytomegalovirus binding to human monocytes induces immunoregulatory gene expression. J.Immunol. **162**:4806-4816

139. **Viswanathan, K., M. S. Smith, D. Malouli, M. Mansouri, J. A. Nelson, and K. Fruh**. 2011. BST2/Tetherin enhances entry of human cytomegalovirus. PLoS.Pathog. **7**:e1002332

140. **Seo, J. Y., R. Yaneva, E. R. Hinson, and P. Cresswell**. 2011. Human cytomegalovirus directly induces the antiviral protein viperin to enhance infectivity. Science **332**:1093-1097

141. **Hansen, S. G., J. B. Sacha, C. M. Hughes, J. C. Ford, B. J. Burwitz, I. Scholz, R. M. Gilbride, M. S. Lewis, A. N. Gilliam, A. B. Ventura, D. Malouli, G. Xu, R. Richards, N. Whizin, J. S. Reed, K. B. Hammond, M. Fischer, J. M. Turner, A. W. Legasse, M. K. Axthelm, P. T. Edlefsen, J. A. Nelson, J. D. Lifson, K. Fruh, and L. J. Picker**. 2013. Cytomegalovirus vectors violate CD8+ T cell epitope recognition paradigms. Science **340**:1237874

142. **Teng, T. S., S. S. Foo, D. Simamarta, F. M. Lum, T. H. Teo, A. Lulla, N. K. Yeo, E. G. Koh, A. Chow, Y. S. Leo, A. Merits, K. C. Chin, and L. F. Ng**. 2012. Viperin restricts chikungunya virus replication and pathology. J Clin.Invest **122**:4447-4460

143. **McGillivary, G., Z. B. Jordan, M. E. Peeples, and L. O. Bakaletz**. 2013. Replication of respiratory syncytial virus is inhibited by the host defense molecule viperin. J Innate.Immun. **5**:60-71

144. **Nasr, N., S. Maddocks, S. G. Turville, A. N. Harman, N. Woolger, K. J. Helbig, J. Wilkinson, C. R. Bye, T. K. Wright, D. Rambukwelle, H. Donaghy, M. R. Beard, and A. L. Cunningham**. 2012. HIV-1 infection of human macrophages directly induces viperin which inhibits viral production. Blood **120**:778-788

145. **Helbig, K. J., N. S. Eyre, E. Yip, S. Narayana, K. Li, G. Fiches, E. M. McCartney, R. K. Jangra, S. M. Lemon, and M. R. Beard**. 2011. The antiviral protein viperin inhibits hepatitis C virus replication via interaction with nonstructural protein 5A. Hepatology **54**:1506-1517

146. **Wang, S., X. Wu, T. Pan, W. Song, Y. Wang, F. Zhang, and Z. Yuan**. 2012. Viperin inhibits hepatitis C virus replication by interfering with binding of NS5A to host protein hVAP-33. J Gen.Virol **93**:83-92

147. **Rolle, S., A. M. De, D. Gioia, D. Lembo, L. Hertel, S. Landolfo, and M. Gariglio**. 2001. The interferon-inducible 204 gene is transcriptionally activated by mouse cytomegalovirus and is required for its replication. Virology **286**:249-255

148. **Hertel, L., A. M. De, B. Azzimonti, A. Rolle, M. Gariglio, and S. Landolfo**. 1999. The interferon-inducible 204 gene, a member of the Ifi 200 family, is not involved in the antiviral state induction by IFN-alpha, but is required by the mouse cytomegalovirus for its replication. Virology **262**:1-8

149. **Schrier, R. D., J. A. Nelson, and M. B. Oldstone**. 1985. Detection of human cytomegalovirus in peripheral blood lymphocytes in a natural infection. Science **230**:1048-1051

150. **Stanier, P., D. L. Taylor, A. D. Kitchen, N. Wales, Y. Tryhorn, and A. S. Tyms**. 1989. Persistence of cytomegalovirus in mononuclear cells in peripheral blood from blood donors. BMJ **299**:897-898

151. **Taylor-Wiedeman, J., P. Sissons, and J. Sinclair**. 1994. Induction of endogenous human cytomegalovirus gene expression after differentiation of monocytes from healthy carriers. J.Virol. **68**:1597-1604

152. **Soderberg-Naucler, C., K. N. Fish, and J. A. Nelson**. 1997. Reactivation of latent human cytomegalovirus by allogeneic stimulation of blood cells from healthy donors. Cell **91**:119-126

153. **Reeves, M. B., P. A. MacAry, P. J. Lehner, J. G. Sissons, and J. H. Sinclair**. 2005. Latency, chromatin remodeling, and reactivation of human cytomegalovirus in the dendritic cells of healthy carriers. Proc Natl Acad Sci U S A **102**:4140-4145

154. **Nogueira, L. G., R. H. Santos, B. M. Ianni, A. I. Fiorelli, E. C. Mairena, L. A. Benvenuti, A. Frade, E. Donadi, F. Dias, B. Saba, H. T. Wang, A. Fragata, M. Sampaio, M. H. Hirata, P. Buck, C. Mady, E. A. Bocchi, N. A. Stolf, J. Kalil, and E. Cunha-Neto**. 2012. Myocardial chemokine expression and intensity of myocarditis in Chagas cardiomyopathy are controlled by polymorphisms in CXCL9 and CXCL10. PLoS.Negl.Trop.Dis. **6**:e1867

155. **Gouwy, M., S. Struyf, H. Verbeke, W. Put, P. Proost, G. Opdenakker, and D. J. Van**. 2009. CC chemokine ligand-2 synergizes with the nonchemokine G protein-coupled receptor ligand fMLP in monocyte chemotaxis, and it cooperates with the TLR ligand LPS via induction of CXCL8. J.Leukoc.Biol. **86**:671-680

156. **de, N. P., C. Chenivesse, J. Gilet, H. Porte, H. Vorng, Y. Chang, A. F. Walls, B. Wallaert, A. B. Tonnel, A. Tsicopoulos, and H. G. Zerwes**. 2006. CCR5 usage by CCL5 induces a selective leukocyte recruitment in human skin xenografts in vivo. J.Invest Dermatol. **126**:2057-2064

157. **Schall, T. J., K. Bacon, K. J. Toy, and D. V. Goeddel**. 1990. Selective attraction of monocytes and T lymphocytes of the memory phenotype by cytokine RANTES. Nature **347**:669-671

ABSTRACT

HUMAN CYTOMEGALOVIRUS US17 LOCUS FINE-TUNES INNATE AND INTRINSIC IMMUNE RESPONSES

by

STEPHEN J. GURCZYNSKI

December 2013

Advisor: Dr. Philip E. Pellett

Major: Immunology and Microbiology

Degree: Doctor of Philosophy

HCMV employs numerous strategies to combat, subvert, or co-opt host immunity. One evolutionary strategy for this involves “capture” of a host gene and then its successive duplication and divergence, forming a gene family, many of which have immunomodulatory activities. The HCMV US12 family consists of ten tandemly arranged sequence-related genes in the unique short region of the HCMV genome (US12-US21). Each gene encodes a protein possessing seven predicted transmembrane domains, and patches of sequence similarity with cellular GPCRs and the bax inhibitor-1 family of anti-apoptotic proteins.

We show that one member, US17, plays an important role during virion maturation. Microarray analysis of cells infected with a recombinant HCMV deleted for US17 (ΔUS17) revealed blunted host innate and interferon responses at early times after infection (12 hpi), a pattern opposite that previously seen in the absence of the immunomodulatory tegument protein pp65 (pUL83). Although ΔUS17 produced equal numbers of infectious particles in fibroblasts compared to parental virus, at equal multiplicities of infection, it produced >3-fold more genome-

containing non-infectious viral particles, and delivered increased amounts of pp65 to newly infected cells.

At later time points (96 hpi) ΔUS17 infected cells displayed aberrant expression of several host ER stress response genes and chaperones, some of which are important for the final stages of virion assembly and egress. Our results suggest that US17 modulates host pathways which control virion composition enabling production of virions that elicit an appropriately balanced host immune response.

AUTOBIOGRAPHICAL STATEMENT

I was born in Dearborn, Michigan in 1981 and have been a native of Michigan all of my life. I attended Divine Child High School and graduated with honors in 1999. After high school I attended the University of Michigan Dearborn where I majored in microbiology. College was my first real introduction to biology and cemented my love for working in a laboratory. After graduating with a B.S. in 2005 I went to work as a research assistant developing recognition substrates for microbial biosensors in the laboratory of Dr. Matthew Jackson at the Wayne State University School of Medicine. This project was multidisciplinary and exposed me to a wide variety of scientific topics from microbiology to chemical engineering. During this time period I also met my wife Laura who has been a great inspiration in my life. When the project ended in 2007 I was left with a choice of what I wanted to do for the rest of my life. Dr. Jackson urged me to apply for the Ph.D. program at the School of Medicine. I joined the laboratory of Dr. Philip Pellett as a Ph. D. candidate in 2008 and have spent the last several years studying human cytomegalovirus cellular interactions, specifically, how HCMV virion protein composition influences the innate immune system. The years building up to the completion of my Ph.D. have been eventful, I've gotten married, had a son, Raymond, bought a house, and just recently successfully defended my Ph. D. thesis. This truly has been the best time of my life and I feel extremely fortunate that my life has taken the path that it has.